Wave-Function-Based Embedding Potential for Ion-Covalent Crystals

I. V. Abarenkov* and M. A. Boyko

Many important properties of crystals are the result of the local defects. However, when one address directly the problem of a crystal with a local defect one must consider a very large system despite the fact that only a small part of it is really essential. This part is responsible for the properties one is interested in. By extracting this part from the crystal one obtains a so-called cluster. At the same time, properties of a single cluster can deviate significantly from properties of the same cluster embedded in crystal. In many cases, a single cluster can even be unstable. To bring the state of the extracted cluster to that of the cluster in the crystal one must apply a so-called embedding potential to the cluster. This article discusses a case study of embedding for ion-covalent crystals. In the case considered, the embedding potential has two qualitatively different components, a long-range (Coulomb), and a short-range. Different methods should be used to generate different components. A number of approximations are used in the method of generating an embedding potential. Most of these approximations are imposed to make the equations and their derivation simple and these approximations can be easily lifted. Besides, the one-determinant approximation for the wave function is used. This is a reasonably good approximation for ion-covalent systems with closed shells, which simplifies the problem considerably and makes it tractable. All employed approximations are explicitly stated and discussed. Every component of generation methods is described in details. The proofs of used statements are provided in a relevant appendix. © 2015 Wiley Periodicals, Inc.

DOI: 10.1002/qua.25041

Introduction

An immediate solution of the Schroedinger equation for a real crystal is impossible due to an enormous number of particles in the system and a complicated system structure. However, a real crystal consists of similar, almost identical, repeating parts. Therefore, one can substitute a real crystal with its model as an infinite system with translational symmetry. This model is usually referred to as a perfect crystal. The first methods which were applied to a perfect crystal problem are: the Wigner–Seitz cell method,[1,2] the tight-binding method,[3,4] the orthogonalized plane wave method,[5] the augmented plane wave method,[6] the Korringa–Kohn–Rostoker method[7,8] and their modifications. There are, at present, a wide variety of methods that can be used to calculate the perfect crystals properties.

However, many technologically important crystal properties are the result of crystal defects and impurities. These defects and impurities break down the perfect crystal translational symmetry. Many of these defects are local and their properties are determined by a comparatively small region of the crystal. Although the actual region is small, it is still part of the large system. There are two general approaches to this problem. One of them uses the well-developed methods of band structure calculations. The system is accordingly transformed to fit these methods. In this approach, a polyatomic system is used as an elementary unit cell of the crystal. This polyatomic system is referred to as a quasimolecule. It is referred to as a quasimolecule, because it is not an isolated molecule but is a fragment of the crystal, although the number and arrangement of atoms in a quasimolecule is similar to that in a real molecule. A large enough part of the crystal around an impurity is selected. This part contains an integer number of quasimolecules carefully arranged to preserve the translational symmetry with translation vectors being the integer number of the initial lattice translation vectors. This large part is referred to as the main region. Calculations are performed for the main region with periodic boundary conditions (the Born–von Karman boundary conditions) imposed on it.

In the simplest case, the main region is one quasimolecule. This is the so-called Cyclic Cluster Model,[9–11] which takes account of translationally equivalent atoms of a quasimolecule. In a 1-D case, it corresponds to a linear molecule bent into a closed chain. In the general case, the main region contains many quasimolecules.

In the case of the crystal defect problem, a crystal with a single defect is replaced by a crystal with periodically situated defects. The unit cell (the quasimolecule) of a new crystal is referred to as a supercell[12,13]; and the method itself is referred to as a supercell approach. The supercell is generated to have defect in its center and to make the distance between defects large enough to minimize defects interaction.

I. V. Abarenkov, M. A. Boyko
Physics Department, St. Petersburg State University, St. Petersburg, Russia E-mail: aiv@pcqnt1.phys.spbu.ru

Contract grant sponsor: Russian Foundation for Basic Research; contract grant number: 15-03-07543.
Contract grant sponsor: St. Petersburg State University; contract grant number: 11.38.261.2014.

Currently, the supercell method is widely applied to crystals with small radius defects.

A quasimolecule can be generated with the help of not only translational symmetry operations, as in the supercell method, but also using point symmetry operations. In the large unit cell (LUC) method,[12,14,15] the unit cell is generated so that one-electron energies, calculated in its Brillouin zone center, correspond to energies at the main important points of the minimal unit cell Brillouin zone. Therefore, the results of LUC calculations can be directly compared with the results of the standard band structure calculations for a perfect crystal.[16–18]

Another approach to the defect crystal problem is to consider the finite system that is part of the infinite crystal. Not being single this part is under the influence of an external potential chosen to minimize the difference between state of the finite system in this potential and state of the same system as part of the infinite crystal. In this approach, the finite part of the crystal is usually referred to as a cluster, the potential is referred to as the embedding potential and the approach itself can be referred to as cluster in the embedding potential method.

The advantage of the cluster approach is the possibility to use the well-developed high-quality methods of molecule electronic structure calculations. However, a single cluster is not an appropriate system. Indeed, single cluster properties depend on the cluster shape. In a single cluster, there are surface states, which are absent in the crystal. When one separates a cluster from the rest of the crystal one has to break some chemical bonds which entails consequent broken bonds saturation. All these problems are absent when one considers a cluster in a properly chosen embedding potential.

In the simplest cases, such as strongly ionic solids for example, an embedding potential can be generated with the help of classical point charges potential. In more complex cases, quantum-mechanical contributions to the embedding potential must be used. All quantum-mechanical embedding potential methods can be divided into two groups: the wave function-based methods and the density functional theory (DFT)-based methods.

In accordance with their name, in the wave function-based methods, the embedding potential is generated using system and subsystems wave functions. For example, in the *ab initio* model potential (AIMP) method the fixed one-electron atomic functions of crystalline environment are used.[19,20] The AIMP embedding potential consists of a point charge potential, a nonpoint charge contribution, that is, a Coulomb potential due to electron density, a quantum-mechanical exchange potential due to the interaction between environment electrons and cluster electrons, and a quantum-mechanical Pauli repulsion contribution due to environment electrons. Although the wave function-based methods are approximate, they are open to systematic improvement. In the DFT-based embedding methods, the frozen density embedding theory (FDE) is used[21–24]; and the Kohn-Sham (KS) DFT one-electron equations for a cluster in the embedding potential are developed by minimizing the total energy of the system, assuming that the crystal environment density is frozen. The DFT-based embedding methods take account of correlation effects. This is an evident advantage of the DFT-based embedding methods. Unfortunately, both the KS and embedding potentials depend on the density functionals whose exact form is unknown. It makes impossible the systematic improvement of DFT-based methods results.

Apart from the methods where Shroedinger equation is used immediately, Green function methods are also applied to the crystal with defect problem, two opposite approaches being employed. In one approach, a crystal with a single defect is considered as a crystal perturbed by a defect,[25–27] in another approach a cluster perturbed by a perfect crystal is considered.[28,29] The later approach is formulated using the linear combination of atomic orbitals (LCAO) and is based on the assumption that molecular cluster density of states projected on the crystal is the same as in the perfect crystal under consideration.

Some point defects produce crystal perturbation in such a large region that corresponding cluster becomes too big for direct quantum-mechanical calculations. A charged defect is an example. However, in many of these cases, the crystal quantum state is changed essentially only in some small inner part of the perturbed region. While the most part of perturbation results from crystal atoms displacement, this displacement is usually too important to be neglected. In these cases, a hybrid quantum mechanic/molecular mechanic approach is used which is known as a QM/MM method suggested by Warshell and Levitt[30,31] for biomolecules investigation. The quantum mechanical (QM) methods are used to calculate a QM cluster (the inner part of the perturbed region). The molecular mechanics (MM) force fields, based on empirical potentials describing small vibrations, van der Waals interactions, and so on are used to calculate cluster environment (the outer part of the perturbed region) and cluster–environment interaction.

The QM/MM method combines quantum mechanical description accuracy and the low computational cost of molecular mechanics; therefore, it is widely used in organic and no-organic systems investigations[32,33] and in solids for modeling defects,[34–36] excitations,[37] properties,[38–40] interfaces,[41] future molecular devices,[42] and so on.

The detailed review of embedding methods can be found in the recently published papers.[43–46]

A comprehensive review of different models applicability for description of the real crystals bulk and surface properties can be found in.[47–49]

In this article, the wave function-based embedding for ion-covalent crystals is considered.

This article outline is the following. First, the embedding is demonstrated in the simple case of one electron in the periodic potential with a single local impurity potential. It is shown that using Green function one can describe the influence of the crystal on the electron in the impurity region as the embedding potential.

Then the ion-covalent crystal electronic structure is considered in the closed shells one-determinant Hartree-Fock (HF) approximation. Here noncanonical localized orbitals are introduced; the division of the crystal into a cluster and cluster

environment is discussed; the environment is divided into a far environment and a near environment; a cluster in crystal molecular orbitals are introduced.

Next, the long-range part of the embedding potential, conditionally named Coulomb embedding, is considered. Usually, the long-range part of embedding potential, for which the far environment is responsible, is modeled by the potential produced by the finite system of point charges. The general method to generate the finite system of charges modeling the infinite point ion crystal potential with any desirable precision and applicable to any lattice is described.

The long-range part of the near environment potential is described next and a simple approximation to it is introduced.

Finally, the short-range part of the embedding potential is described considering both the single cluster and the same cluster as part of the crystal. A common quantum-mechanical stationary state problem is stated as follows: given the external potential, calculate a system molecular orbitals and energies. At the same time, an inverse problem can be considered as well: given the molecular orbitals and energies, generate an external potential that will produce these orbitals and energies. Short-range embedding potential generation is a second type problem. In this section of the article, a particular method is described to generate a cluster in finite crystal molecular orbitals and energies. Then, assuming that all occupied and virtual molecular orbitals of the cluster are eigenfunctions of the same equation (one-determinant HF or DFT KS), it is shown that the potential with the following property can be made: the self-consistent field calculations of a cluster in this potential produce exactly the predefined orbitals and energies of the cluster in the crystal.

Each part is described in details and the proof of every used statement is provided in a relevant appendix.

One electron in the periodic potential with single local impurity

In this section, the embedding approach is considered in application to the case of one electron in the potential of particular form. The potential was chosen to model a single local impurity in a perfect crystal. This potential is assumed to be the sum of a periodic potential $V_0(\mathbf{r})$ (modeling the perfect crystal) and a finite radius local potential $V(\mathbf{r})$ (modeling the impurity). The finite radius potential means that there exists a radius R such that the potential $V(\mathbf{r})$ is equal to zero outside the radius R sphere. The stationary bounded state of one electron in the potential described above is considered. A corresponding wave function is the solution of the Schroedinger equation

$$\left(-\frac{1}{2}\Delta + V_0(\mathbf{r}) + V(\mathbf{r})\right)\psi(\mathbf{r}) = E\,\psi(\mathbf{r}) \tag{1}$$

with zero boundary conditions at the infinity. Equation (1) is valid in the whole infinite space. However, in the case considered, the problem can be confined only to the impurity region. To do this, one can use a closed surface S to divide

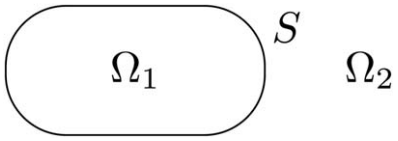

Figure 1. The closed surface S divided the total space into subspaces Ω_1 and Ω_2.

the whole space Ω into two subspaces Ω_1 and Ω_2, $\Omega=\Omega_1\oplus\Omega_2$, the subspace Ω_2 being selected so that the impurity potential is equal to zero in it (Fig. 1). Then boundary conditions at the surface S can be generated so that a properly normalized solution of Eq. (1) in the subspace Ω_1 with the said boundary condition will coincide in Ω_1 with the solution of the same Eq. (1) in the whole space with zero boundary conditions at the infinity. In other words, the boundary conditions can be transferred from the infinity to the surface S.

It can be done with the help of the periodic potential Green function G_0[50,51] (Appendix A). In addition to the Green function G_0, it is necessary to define the surface inverse G_0^{-1} of G_0 as

$$\int_S G_0^{-1}(\mathbf{r}_s, \mathbf{r}_s''; E)\, G_0(\mathbf{r}_s'', \mathbf{r}_s'; E)\, d^2 r_s'' = \delta^2(\mathbf{r}_s, \mathbf{r}_s').$$

The subscript s means that $\mathbf{r}_s$ belongs to the surface S. With G_0 and G_0^{-1}, the function $U(\mathbf{r}_s, \mathbf{r}_s'; E)$ of surface variables $\mathbf{r}_s$, $\mathbf{r}_s'$ and energy E can be defined as

$$U(\mathbf{r}_s, \mathbf{r}_s'; E) = G_0^{-1}(\mathbf{r}_s, \mathbf{r}_s'; E) + \frac{1}{2}\int_S G_0^{-1}(\mathbf{r}_s, \mathbf{r}_s''; E)\frac{\partial}{\partial \boldsymbol{n}_s'} G_0(\mathbf{r}_s'', \mathbf{r}_s'; E)\, d^2 r_s''.$$

In the Appendix A, it is shown that any solution of Eq. (1) with zero at infinity boundary conditions satisfies the equation

$$\frac{1}{2}\frac{\partial}{\partial \boldsymbol{n}_s}\psi(\mathbf{r}_s) = \int_S U(\mathbf{r}_s, \mathbf{r}_s'; E)\,\psi(\mathbf{r}_s')\, d^2 r_s'. \tag{2}$$

This equation is the nonlocal form of an ordinary boundary condition connecting the value of a function's derivative at the boundary and the value of the function at the boundary. Therefore, if one needs the wave function in the impurity region Ω_1 only, one can solve Eq. (1) in Ω_1 space

$$\left(-\frac{1}{2}\Delta + V_0(\mathbf{r}) + V(\mathbf{r})\right)\psi(\mathbf{r}) = E\,\psi(\mathbf{r}), \qquad \mathbf{r}\in\Omega_1 \tag{3}$$

imposing (2) as the boundary condition.

Consequently, in the case of one electron in the considered potential, the problem of the electronic structure calculation in the whole infinite space can be turned into a problem in the finite space Ω_1, the embedding being done by imposing the boundary conditions on the space Ω_1 outer surface S.

In the electronic structure calculations, it is always useful and convenient to know the energy functional corresponding to the wave function equation. In the case of one electron in

the considered potential, the energy functional with a trial function $\varphi(\boldsymbol{r})$, depending on $\boldsymbol{r}$ in the space Ω_1 and on the surface S only, is

$$W[\varphi]=\int\limits_{\Omega_1}\left\{\frac{1}{2}|\nabla\varphi(\mathbf{r})|^2+V_0(\mathbf{r})|\varphi(\mathbf{r})|^2+V(\mathbf{r})|\varphi(\mathbf{r})|^2\right\}d^3r - \int\limits_S\int\limits_S \varphi^*(\mathbf{r}_s)\,U(\mathbf{r}_s,\mathbf{r}_s';E)\,\varphi(\mathbf{r}_s')\,d^2r_s'd^2r_s. \tag{4}$$

The corresponding normalization condition is

$$N[\varphi]=\int\limits_{\Omega_1}|\varphi(\mathbf{r})|^2\,d^3r=1.$$

To obtain the wave function equations, one can use either the constrained variation of the functional $W[\varphi]$ with an additional condition $N[\varphi]=1$, or the unconstrained variation of the functional $W[\varphi]-\lambda N[\varphi]$ with a Lagrange multiplier λ. In the latter case, it is expedient to use the equation

$$\int\limits_{\Omega_1}|\nabla\varphi(\mathbf{r})|^2\,d^3r=-\int\limits_{\Omega_1}\varphi^*(\mathbf{r})\Delta\varphi(\mathbf{r})\,d^3r+\int\limits_S\varphi^*(\mathbf{r}_s)\frac{\partial}{\partial\boldsymbol{n}_s}\varphi(\mathbf{r}_s)d^2r_s$$

and rewrite the functional in the form

$$W[\varphi]-\lambda N[\varphi]=\int\limits_{\Omega_1}\varphi^*(\mathbf{r})\left\{-\frac{1}{2}\Delta+V_0(\mathbf{r})+V(\mathbf{r})-\lambda\right\}\varphi(\mathbf{r})\,d^3r + \int\limits_S\varphi^*(\mathbf{r}_s)\left\{\frac{1}{2}\frac{\partial}{\partial\boldsymbol{n}_s}\varphi(\mathbf{r}_s)-\int\limits_S U(\mathbf{r}_s,\mathbf{r}_s';E)\,\varphi(\mathbf{r}_s')\,d^2r_s'\right\}d^2r_s. \tag{5}$$

Variation of the first term in the right-hand side of (5) results in Eq. (3) for the wave function and variation of the second term results in the boundary conditions (2). Therefore, boundary conditions (2) are the natural boundary conditions for functional (5).

Using Eq. (4), one can write the equation for the electron in single local impurity potential energy

$$E=\int\limits_{\Omega_1}\left\{\frac{1}{2}|\nabla\psi(\mathbf{r})|^2+V_0(\mathbf{r})|\psi(\mathbf{r})|^2+V(\mathbf{r})|\psi(\mathbf{r})|^2\right\}d^3r - \int\limits_S\int\limits_S\psi^*(\mathbf{r}_s)\,U(\mathbf{r}_s,\mathbf{r}_s';E)\,\psi(\mathbf{r}_s')\,d^2r_s'd^2r_s,\qquad \int\limits_{\Omega_1}|\psi(\mathbf{r})|^2\,d^3r=1.$$

This equation shows that the value

$$E_{\text{embd}}=-\int\limits_S\int\limits_S\psi^*(\mathbf{r}_s)\,U(\mathbf{r}_s,\mathbf{r}_s';E)\,\psi(\mathbf{r}_s')\,d^2r_s'd^2r_s$$

can be considered as the embedding potential energy and the quantity $U(\mathbf{r}_s,\mathbf{r}_s';E)$ as the nonlocal embedding potential core.

Two points should be mentioned here. First, boundary conditions are determined by the potential $V_0(\boldsymbol{r})$ of the perfect system and does not depend on a particular impurity potential. Hence for given perfect system the function U can be calculated only once and be used for different impurities. Second, complications may arise if the energy will be determined in the process of solving the equation. These complications are due to the fact that the energy E enters not only the equation directly, but also the boundary conditions through the function U.

Ion-covalent crystal

In this section, the electronic structure of an ion-covalent crystal is discussed. Instead of the infinite crystal approximation and localized Wannier functions[52] approach, the large finite crystal will be considered here within closed shells one-determinant HF approximation. Similar results can be obtained with a KS DFT approximation. In the closed shells case, the standard HF equation for one-electron orbitals $\psi_i(\boldsymbol{r})$ (both occupied and virtual) is

$$\hat{F}(\boldsymbol{r})\psi_i(\boldsymbol{r})=\varepsilon_i\psi_i(\boldsymbol{r}). \tag{6}$$

where $\hat{F}$ is Fock operator of the finite crystal and ε_i are one-electron energies (ionization potentials). All one-electron orbitals $\psi_i(\boldsymbol{r})$ are orthonormal eigenfunctions of the same operator. They are usually referred to as canonical orbitals and Eq. (6) is referred to as canonical HF equation. The Fock operator is the sum

$$\hat{F}(\boldsymbol{r})=\hat{T}(\boldsymbol{r})+\hat{V}(\boldsymbol{r})+\hat{J}(\boldsymbol{r})-\hat{K}(\boldsymbol{r})$$

of kinetic energy operator $\hat{T}(\boldsymbol{r})$, electron–nucleus interaction energy operator $\hat{V}(\boldsymbol{r})$, Coulomb operator $\hat{J}(\boldsymbol{r})$

$$\hat{J}(\boldsymbol{r})=\int\frac{\rho(\boldsymbol{r}'|\boldsymbol{r}')}{|\boldsymbol{r}-\boldsymbol{r}'|}d\boldsymbol{r}',$$

and exchange operator $\hat{K}(\boldsymbol{r})$

$$\hat{K}(\boldsymbol{r})f(\boldsymbol{r})=\frac{1}{2}\int\frac{\rho(\boldsymbol{r}|\boldsymbol{r}')f(\boldsymbol{r}')}{|\boldsymbol{r}-\boldsymbol{r}'|}d\boldsymbol{r}',$$

where the electron density matrix of the crystal is

$$\rho(\boldsymbol{r}|\boldsymbol{r}')=2\sum_{i=1}^{N}\psi_i(\boldsymbol{r})\psi_i^*(\boldsymbol{r}'), \tag{7}$$

where N is the number of occupied orbitals (each orbital is occupied by two electrons).

For the large enough finite crystal, the properties of its inner part, which is far from crystal boundaries, are almost independent of the crystal size. Besides, properties of two similar inner parts, which can be obtained one from the other by a crystal translational symmetry operation, are almost identical. Hence a comparatively small inner part of a finite crystal can provide information about the state of the whole crystal. This inner part is usually referred to as a cluster and the rest of the crystal—as a cluster environment.

At the same time, the crystal canonical occupied orbitals $\psi_i(\boldsymbol{r})$ are spread over the whole crystal volume. Therefore, all crystal canonical orbitals must be used to describe even small cluster properties. However, Eq. (6) can be transformed to have linear combinations of canonical orbitals (separately occupied and virtual) for its solution instead of the canonical orbitals themselves. The linear combinations of canonical orbitals are usually referred to as noncanonical orbitals. The particular noncanonical orbitals divided into two groups can be obtained, each group being localized in different regions. The orbitals of one group are large in the cluster region and are small in the cluster environment region; the orbitals of another group are small in the cluster region and are large in the cluster environment region. The orbitals localized in the cluster (first group orbitals) can be considered as a cluster in crystal orbitals; and the system of equations for them can be considered as an equation for a cluster in crystal.

The above transformation of orbitals into the localized ones is based on one-determinant approximation for the total wave function and on the fact that the determinant with particular orbitals differs only by a constant factor from the determinant in which instead the particular orbitals their linear combinations are used, providing that orbitals transformation is not singular. Canonical HF equations (6) are Euler–Lagrange variational principle equations obtained from the quantum system total energy minimization subject to auxiliary conditions of orbital orthonormality. These conditions are taken into account with the help of Lagrange multipliers. The Lagrange multipliers make a $N\times N$ matrix, where diagonal multipliers are responsible for orbitals normalization, and nondiagonal multipliers are responsible for orbitals orthogonalization. However, if (in the case considered), the nondiagonal multipliers are set equal to zero then each equation in the Euler–Lagrange system of equations is the eigenfunction and eigenvalue equation for some operator; and the operator is the same in all equations. Thus, all occupied orbitals are eigenfunctions of one operator; and in the case of nondegenerate eigenvalues, they are automatically orthogonal. In the case of degenerate eigenvalue, the corresponding eigenfunctions can be made orthonormal with an appropriate linear transformation. Therefore, the simplest choice of nondiagonal multipliers to make orbitals orthogonal is to set them equal to zero. This choice of nondiagonal Lagrange multipliers was adopted in Eq. (6) derivation.

However, orthogonality requirement is too strong. In fact, in the corresponding variational principle, the only necessary condition, which should be imposed on orbitals, is their linear independence. In this case, instead Eqs. (6), the following system of equations for occupied orbitals can be obtained from the variational principle[53] (Appendix B)

$$\hat{F}\varphi_j(\boldsymbol{r})=\hat{\rho}\hat{F}\hat{\rho}\varphi_j(\boldsymbol{r}),\qquad j=1,\ldots,N, \tag{8}$$

where $\hat{\rho}$ is the integral operator with the density matrix $\rho(\boldsymbol{r}|\boldsymbol{r}')$ for kernel

$$\hat{\rho}f(\boldsymbol{r})=\int\rho(\boldsymbol{r}|\boldsymbol{r}')f(\boldsymbol{r}')d\boldsymbol{r}'.$$

In the general case, the equation for the density matrix is

$$\rho(\boldsymbol{r}|\boldsymbol{r}')=\sum_{j,k=1}^{N}\varphi_j(\boldsymbol{r})(S^{-1})_{jk}\varphi_k^*(\boldsymbol{r}'), \tag{9}$$

where

$$S_{jk}=\int\varphi_j^*(\boldsymbol{r})\varphi_k(\boldsymbol{r})d\boldsymbol{r}$$

is the orbitals overlap integrals matrix. In the case of orthonormal orbitals $\psi_j(\boldsymbol{r})$, the overlap matrix is equal to the unit matrix and Eq. (7) is obtained. It should be noted that the density matrix (7) is invariant under any unitary transformation of occupied orbitals $\psi_j(\boldsymbol{r})$ and the density matrix (9) is invariant under any nonsingular transformation of occupied orbitals $\varphi_j(\boldsymbol{r})$.

Equation (8) can be considered as an eigenvalue and eigenfunction equation

$$\left(\hat{F}-\hat{\rho}\hat{F}\hat{\rho}\right)\varphi_j(\boldsymbol{r})=0,\qquad j=1,\ldots,N$$

with one operator $\hat{F}-\hat{\rho}\hat{F}\hat{\rho}$ and one N-times degenerate eigenvalue equal to zero. Due to this degeneracy, any linear combination of Eq. (8) eigenfunctions is also the eigenfunction of Eq. (8). Equation (8) is the general equation satisfied by any system of N valid occupied orbitals. It should also be noted that although in the equation for the noncanonical orbitals derivation the orthogonality conditions were lifted, it does not mean that the noncanonical orbitals are necessarily nonorthogonal. Indeed, any unitary transformed canonical orbitals are the noncanonical orbitals, and they are still orthonormal.

The orbitals of a cluster in crystal are the particular noncanonical orbitals of a ion-covalent crystal localized in the cluster. There are many ways to achieve orbitals localization.[54,55] One of the simplest ways is to consider the orbital $\varphi(\boldsymbol{r})$ as localized the in cluster that brings maximum to the integral

$$W=\int\varphi^*(\boldsymbol{r})w(\boldsymbol{r})\varphi(\boldsymbol{r})d\boldsymbol{r},$$

where $w(\boldsymbol{r})$ is some positive function equal to zero outside the cluster. Different equations for the functional W can be used for different criteria of localization. It is possible (Appendix B) to derive equations for orbitals $\varphi_j(\boldsymbol{r})$ which are solutions to the Eq. (8), normalized to 1, and bring extremum to the additional functional W

$$W=\sum_{j=1}^{N}\int\varphi_j^*(\boldsymbol{r})\hat{w}\varphi_j(\boldsymbol{r})d\boldsymbol{r}.$$

These equations are

$$\left(\hat{F}+\hat{\rho}\left(\hat{w}-\hat{F}\right)\hat{\rho}\right)\varphi_i(\boldsymbol{r})=\lambda_i\varphi_i(\boldsymbol{r}). \tag{10}$$

Equations (10) can be written in the form

$$\left(\hat{F}+\hat{\rho}\hat{A}\hat{\rho}\right)\varphi_i(\boldsymbol{r})=\lambda_i\varphi_i(\boldsymbol{r}), \tag{11}$$

known as Adams–Gilbert equations.[56,57] Here,

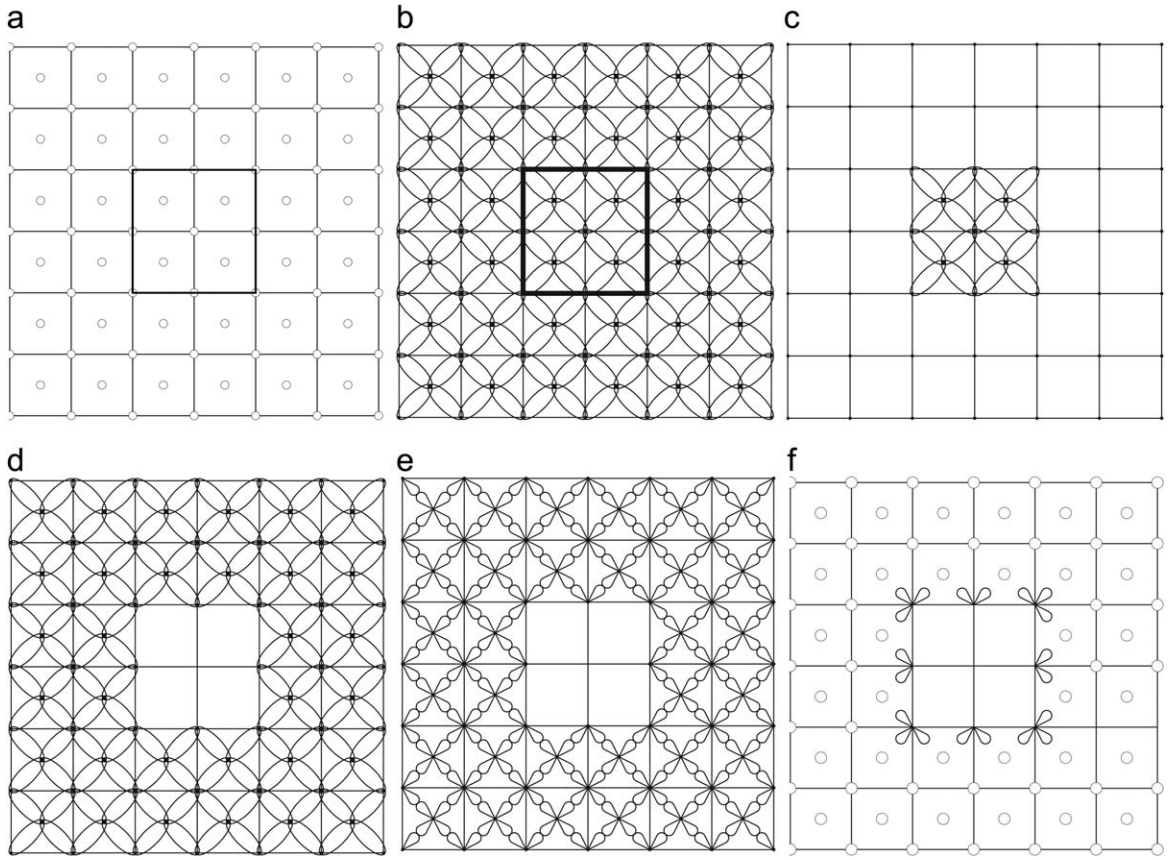

Figure 2. a) The crystal with atoms of two types and square lattice. The cluster is marked by bold lines. b) The same crystal as a collection of bonds. The cluster is marked by bold lines. c) Cluster as a collection of bonds. d) Cluster environment as a collection of bonds. e) Cluster environment as a collection of directed orbitals. f) Cluster environment as a collection of inner atoms (circles) and directed orbitals at the cluster border.

$$\hat{A} = \hat{w} - \hat{F}.$$

With different operators $\hat{A}$ one can obtain orbitals localized in cluster, atoms, or bonds. Orbitals in crystal localization methods are discussed in details in [54,55]. Application of the Adams–Gilbert method to an MgO crystal is given in [58].

In the perfect ion-covalent crystal with closed shells, the atomic core orbitals, the bonds between nearest neighbors, and the lone-pairs (if any) can be considered as the most appropriate doubly occupied noncanonical localized orbitals. One of the practical methods of localization in this case is the following: it is always possible to define the region that a particular localized orbital should occupy. In this region, a set of well-localized basis functions can be generated, and a projector onto this set can be made. A matrix of the projector can be calculated using as basis the crystal occupied canonical orbitals. This matrix eigenvector, which corresponds to the largest eigenvalue modulus, provides the coefficients of the localized on cluster noncanonical orbital expansion over the canonical crystal orbitals. Note, that standard atomic bases used in the electronic structure calculations may be inconvenient to use as the basis for localization, because the overlap of different atoms bases can be too large.

In what follows, a valence electrons only approximation is adopted for simplicity. In this approximation, all atomic core electrons are taken into account with the help of atomic core pseudopotentials (ECP—the effective core potentials). In the case of a finite crystal, the number of valence electrons is strictly defined: it should be double the number of occupied orbitals inside a finite crystal. The cluster in the crystal should be chosen such that both the cluster and the cluster environment were the closed shells systems. Therefore, the border between the cluster and the cluster environment should be drawn so as to break no bonds and to leave no bonds entirely at the border. It means that the border between the cluster and the cluster environment should pass through atoms and there should be no nearest neighboring atoms at the border.

The crystal division into the cluster and the cluster environment is schematically shown in Figure 2 in the 2-D case. Figure 2a shows a crystal represented as a periodic array of atoms; the rectangular part at the figure center marks the selected cluster. Figure 2b shows a crystal represented as a collection of diatomic bonds. The cluster border passes through atoms. There are no bonds cut by the cluster border, and there are no bonds at the border. Figure 2c shows a cluster as a collection of bonds, while Figure 2d shows a cluster environment represented as a collection of bonds.

If a cluster is selected and occupied bond orbitals belonging to the cluster are calculated as noncanonical orbitals of the crystal, then cluster in the crystal functional space of occupied orbitals is found, and it can be considered as given. The problem is to generate an embedding potential so that occupied orbitals of the cluster in the embedding potential span the given functional space.

When considering an embedding potential, it is convenient to generate its long-range part using an electrostatic potential produced by the cluster environment, its nuclear charges, and its bonds electron density. To avoid unnecessary complications, it is assumed that the crystal contains atoms of only two types, Types 1 and 2 (one is cation and the other is anion), and all bonds of the crystal are similar. In the general case, the approach is the same but the resulting equations are rather elaborated.

Each bond orbital can be considered as one that is made by directed orbitals of the two nearest neighboring atoms (see Fig. 2e for the 2-D case). Each bond density contributes charges to Types 1 and 2 atoms of the bond. These charges will be denoted as ω_1 and ω_2. The bond contains two electrons, so $\omega_1+\omega_2=-2$. In the perfect crystal, m_1 bonds are attached to the Type 1 atom, and m_2 bonds are attached to the Type 2 atom. Thus, in the perfect crystal charges

$$e_1=Z_1+m_1\omega_1, \qquad e_2=Z_2+m_2\omega_2, \tag{12}$$

are assigned to the Types 1 and 2 atoms, where Z_1 and Z_2 are nuclear charges of Types 1 and 2 atoms. One of the charges, say ω_1 (or e_1), can be considered as a free parameter either to adjust the known values of crystal ionic charges (if reliable information about ionic charges exists), or as an adjusting parameter in embedding potential generation.

The cluster environment can be divided into two components. One component consists of all nuclear charges of atoms not belonging to the cluster and of all bonds in which no atoms belong to the cluster. This component will be referred to as the far environment. Another component consists of all directed orbitals attached to the cluster border atoms and directed outward the cluster (Fig. 2f). This component will be referred to as the near environment.

The charges of the far and near environment produce the potential the long-range part of which will be referred to as the Coulomb embedding potential. It will be considered in the next section.

Coulomb embedding

In this section, the long-range part of a cluster embedding potential is considered separately for the far and for the near cluster environment discussed in the previous section. For this part of an embedding potential the short name "Coulomb embedding" is used although only a point charges potential is considered here; the nonpoint correction to the potential attributed to a short-range potential will be considered later. A perfect point ion lattice potential will be considered first.

Point ion lattice potential. The point ion lattice potential of the perfect lattice can be written as

$$V(\boldsymbol{r})=\sum_{\ell}\sum_{j=1}^{n_0}\frac{e_j}{|\boldsymbol{r}-\boldsymbol{R}_\ell-\boldsymbol{\rho}_j|}, \qquad \boldsymbol{R}_\ell=\ell_1\boldsymbol{a}_1+\ell_2\boldsymbol{a}_2+\ell_3\boldsymbol{a}_3, \tag{13}$$

where $\boldsymbol{a}_1$, $\boldsymbol{a}_2$, $\boldsymbol{a}_3$ are the elementary translation vectors, $\boldsymbol{R}_\ell$ is the lattice vector, e_j and $\boldsymbol{\rho}_j$ are the charge and position vector of jth atom in the unit cell, n_0 is the number of atoms in the unit cell.

The common practice is to consider the sum in (13) as an infinite series over all lattice sites. However, with infinite series there arise a convergence problem complicated by the three-dimensionality of the series considered. In a 1-D series, there is a predefined order of summation: a term with an index increased by 1 should be added with each next step. There are three types of series in a 1-D case. The first type includes the series for which the series of absolute values of terms converges. These series are referred to as absolutely convergent. The sum of absolutely convergent series does not depend on the summation order. The second type includes the series that is convergent, but the series of absolute values of terms is divergent. These series are referred to as conditionally convergent. The sum of conditionally convergent series depends on the order of summation and, according to the Riemann series theorem, for any real number, there exists the order of summation with which the series converges to this number. The third type includes the divergent series.

In a 3-D case, there is no predefined order of summation; so there are only two types of 3-D series, convergent and divergent, corresponding to whether the series of absolute values is convergent or not.

Infinite series (13) is divergent because the sum of absolute values of its terms is infinite. At the same time, in any solid state electronic structure calculations, series (13) is dealt with as 1-D, the order of summation being defined by the calculation program. Indeed, even in the case of multiprocessor calculations, the sum is calculated by adding one number at a time. However, the employed 1-D series is conditionally convergent, so one can obtain different results using different calculation programs. It would be much better to use from the very beginning an absolutely convergent series for the crystal potential. In other words, it is desirable to find the proper order of summation for the crystal potential series and fix it, the procedure known as diverging series regularization.

Considering a crystal potential, it is worth noting that in reality there is no such thing as an infinite periodic atomic system. This is simply a mathematical model introduced to make practical calculations of atomic systems with an extremely large number of atoms by changing a large finite sum into an infinite sum for which there exists an exact closed form.

To find the proper order of summations, one can try various rearrangements in the infinite series in Eq. (13) for the point lattice potential, taking into account the real system properties to obtain physically sound results. There are two rearrangements proposed about a hundred years ago. One, proposed by Madelung[59] can be referred to as regrouping. According to this rearrangement, the electrostatic potential of the lattice is considered as a sum of potentials in which each potential is produced by a group of atoms and not by a single atom. Consider the finite group of γ atoms with charges q_j and position vectors $\boldsymbol{d}_j$. It is assumed that being translated with all translation vectors $\boldsymbol{D}_k$, the group will reproduce an infinite lattice. The group electrostatic potential is

$$U(\boldsymbol{r})=\sum_{j=1}^{\gamma}\frac{q_j}{|\boldsymbol{r}-\boldsymbol{d}_j|}, \tag{14}$$

and the infinite lattice potential can be written as

$$V(\boldsymbol{r})=\sum_{k}U(\boldsymbol{r}-\boldsymbol{D}_k), \tag{15}$$

where $\boldsymbol{D}_k$ are the position vectors of the translated group. The group of atoms should be carefully selected to produce absolutely convergent series (15), preferably with fast convergence. In principle, several different groups can be used in the regrouping approach.

Another rearrangement was proposed by Ewald[60] (Appendix C). In this approach, a special form of potential is derived for the potential produced by the finite system of point charges. Then the equation obtained for the finite system of charges is applied to the infinite periodical system of charges and the point ion lattice potential $V(\mathbf{r})$ is obtained as sum of two absolutely convergent series

$$V(\mathbf{r}) = V_1(\mathbf{r}) + V_2(\mathbf{r}), \tag{16}$$

where

$$V_1(\mathbf{r})=\frac{\pi}{\Omega G^2}\sum_{m}^{\prime}\sum_{j=1}^{n_0}e_j e^{i(\mathbf{g}_m,\mathbf{r}-\boldsymbol{\rho}_j)}\frac{e^{-v_m}}{v_m}, \qquad v_m=\frac{g_m^2}{4G^2},$$

$$V_2(\mathbf{r}) = \sum_{k}\sum_{j=1}^{n_0}e_j\frac{erfc(G|\mathbf{r}-\mathbf{R}_k-\boldsymbol{\rho}_j|)}{|\mathbf{r}-\mathbf{R}_k-\boldsymbol{\rho}_j|}, \tag{17}$$

where $\mathbf{g}_m$ is the reciprocal lattice vector and G is the positive parameter controlling the rate of convergence in sums over direct and reciprocal lattices. The potential $V(\boldsymbol{r})$ value does not depend on G.

Equations (16) and (17) are in fact the regularization of the infinite lattice potential series and not its evaluation because the summation and integration operations were interchanged at one stage of these equations derivation [from Equation (C.1) to (C.3), see Appendix C] which is justified in cases of a finite sum and uniformly convergent series only. The initial infinite series for the periodic system of charges is divergent and the said summation and integration operations interchange is not valid. However, the Ewald equation for the potential was found to produce reasonable results, it is simple enough for calculations, and it can be applied to any perfect lattice. Therefore, the Ewald potential is widely used in solid state physics.

Contrary to the Ewald method, which is fixed, different groups of atoms can be used in the regrouping method. Therefore, different approximations can be made with the help of the regrouping method. Since the number of charges in the group is finite, the group potential $U(\boldsymbol{r})$ (14) decreases with increasing r. If a group is selected so that U decreases as $1/r^4$ or faster, then the series in (15) will be absolutely convergent. Indeed, assume that U decreases as $1/r^{4+\alpha}$ with $\alpha > 0$. Potential (15) can be written as a sum of two terms

$$V(\boldsymbol{r})=\sum_{D_k\le R}U(\boldsymbol{r}-\boldsymbol{D}_k)+\sum_{D_k>R}U(\boldsymbol{r}-\boldsymbol{D}_k).$$

The first sum here is finite and for the second sum the following estimation

$$\sum_{D_k>R}|U(\boldsymbol{r}-\boldsymbol{D}_k)| \sim \int_{R}^{\infty}\frac{1}{D^{4+\alpha}}D^2dD \sim \frac{1}{R^{1+\alpha}} \tag{18}$$

shows that the second sum tends to zero with increasing R. Hence, the series in (13) is absolutely convergent.

The group potential U will decrease as $1/r^4$ if the group multipole moments of zero, first, and second order (the charge, dipole, quadrupole, and quadrupole trace) were equal to zero. The convergence will be faster [the sum (18) will decrease faster with increasing R] if higher multipole moments of the group will be equal to zero as well.

Different groups were used in the regrouping method containing integer and fractional charges situated at lattice sites and at artificial sites.[61,62] Constrains can be set[63] within the regrouping method in the case of a perfect lattice to ensure the constant (independent on r) difference between Ewald potential and potential calculated with the regrouping method.

In the regrouping method with a unit cell as a group, the importance of the unit cell dipole and quadrupole moments was understood a long time ago. The unit cell with zero moments for $\ell=0,1,2$ was generated in[64] for three cubic crystals. The unit cell with zero moments up to $\ell=4$ including was generated for several particular crystals in[65]. In papers[66,67], the problem of the unit cell dipole moment and its relation to the crystal surface reconstruction was analyzed in details. It was shown in[63] that if the charge and dipole moment of the unit cell are equal to zero and the quadruple moment is not zero, then the value of the potential depends on the summation region shape.

The electrostatic potential calculation for imperfect lattices, especially for complex lattices with a large atomic basis, can be a problem. One possible approach is to calculate the perfect lattice potential with the Ewald method and add to it the difference between the potential produced by the defect region and the potential produced by the corresponding region of the perfect lattice. Unfortunately, this method requires the Ewald potential calculation in many points. The amount of calculations can be reduced[68] if unit cells will be accumulated around the local defect in the form of a parallelepiped and distant atoms charges, especially the charges at the parallelepiped corner regions, are adjusted to reproduce the Ewald potential at important lattice sites. However, the potential produced by the spherical inner part of the parallelepiped diverges with the increase of the parallelepiped size and this creates problems with controlling the accuracy of potential approximation.

Unit cell for the point ion lattice potential. The advantage of the regrouping method is in the fact that it can be applied both to the perfect lattice and to the lattice with defect. The

key point in this method is group selection. The simplest group is a perfect lattice unit cell. The total charge of this group is equal to zero due to the crystal electroneutrality. At the same time, the dipole and quadrupole moments of the unit cell can be equal to zero only in some particular cases with high-point symmetry. Therefore, in the general case, the conventional unit cell cannot be used as a proper group. However, it was shown in[69] that the unit cell, complemented by a number of additional charges, can be a simple and convenient group resulting in absolute convergent series for the point lattice potential for any lattice.

Consider a group with the following properties

1. The group contains all charges of the original perfect lattice unit cell.
2. The group contains additional charges at several specifically chosen lattice sites.
3. Being translated with all possible translation vectors of the original lattice the group reproduces the original lattice.
4. All the lowest multipole moments of the group up to the ℓ-th moment including are equal to zero.

Any group with the above properties and $\ell \geq 2$ will be referred to as an LP unit cell (a unit cell for the lattice potential). The LP unit cell reproduces the original lattice. Used in Eq. (15), it also results in absolutely convergent series for the potential. The LP unit cell differs from the conventional unit cell and the difference is the following. Different atoms of the conventional unit cell translated with different translation vectors occupy different lattice sites, and only one atom in the conventional unit cell contributes charge to a particular atom in the lattice. At the same time, different atoms of the LP unit cell, translated with different translation vectors, can occupy the same lattice site and, in general, several atoms of the LP unit cell contribute charge to a particular atom in the lattice.

To generate an LP unit cell, one can use simple geometrical considerations. The multipole moments of an LP unit cell are

$$Q(m_1,m_2,m_3)=\sum_{j=1}^{\gamma} q_j\, d_{jx}^{m_1}\, d_{jy}^{m_2}\, d_{jz}^{m_3}, \qquad 0 \leq m_1,m_2,m_3,$$

where q_j and $\boldsymbol{d}_j$ are the LP unit cell charge value and position vector and γ is the number of charges. Each component of mth multipole moment corresponds to three non-negative integers, m_1, m_2, m_3, and can be considered as a point with three integer Cartesian coordinates m_1, m_2, m_3. For each component of mth multipole moment one has

$$m_1+m_2+m_3=m.$$

Therefore, points corresponding to all components of the mth moment can be considered as integer points in the triangle with vertices $(m,0,0)$, $(0,m,0)$, and $(0,0,m)$. The components of all moments up to ℓth including correspond to integers m_1, m_2, m_3 in the range

$$0 \leq m_1,m_2,m_3, \qquad m_1+m_2+m_3 \leq \ell. \tag{19}$$

Hence, they can be considered as integer points in the tetrahedron with vertexes at points (0, 0, 0), $(\ell,0,0)$, $(0,\ell,0)$, $(0,0,\ell)$. In what follows the set of triads (m_1,m_2,m_3) in the range (19) will be denoted as T_ℓ. The number of triads in the set T_ℓ is

$$N_\ell=\frac{1}{6}(\ell+1)(\ell+2)(\ell+3).$$

It is equal to the number of integer points in the mentioned above tetrahedron.

To generate the LP unit cell, the N_ℓ multipole moments must be annulled. At the same time, each component of multipole moment is linear combinations of charges. Therefore, to annul N_ℓ moments one can use N_ℓ additional charges. It is expedient to put additional charges $e(n_1,n_2,n_3)$ at lattice points

$$\boldsymbol{d}(n_1,n_2,n_3)=n_1\boldsymbol{a}_1+n_2\boldsymbol{a}_2+n_3\boldsymbol{a}_3, \qquad n_1,n_2,n_3 \in T_\ell, \tag{20}$$

where integers n_1, n_2, n_3 make the same tetrahedron as integers m_1, m_2, m_3 of the multipole moments. Then the values of additional charges can been found from the system of equations

$$Q_0(m_1,m_2,m_3)+\sum_{n_1,n_2,n_3\in T_\ell} e(n_1,n_2,n_3)\times(d_x(n_1,n_2,n_3))^{m_1} (d_y(n_1,n_2,n_3))^{m_2}(d_z(n_1,n_2,n_3))^{m_3}=0, \qquad m_1,m_2,m_3 \in T_\ell, \tag{21}$$

where

$$Q_0(m_1,m_2,m_3)=\sum_{j=1}^{n_0} e_j\, \rho_{jx}^{m_1}\, \rho_{jy}^{m_2}\, \rho_{jz}^{m_3},$$
$$m_1+m_2+m_3=m.$$

are multipole moments of the original unit cell. In this equation, n_0 is the number of charges in the original unit cell, e_j and ρ_j are the value and position vector of jth charge in the original unit cell. A direct solution to the system (21) with standard routines is not convenient because the equation matrix $d_x^{m_1}\, d_y^{m_2}\, d_z^{m_3}$ could be ill-defined. Indeed, the matrix element is equal to 1 if $m_1=m_2=m_3=0$. At the same time, the equation matrix contains elements proportional to ℓ^ℓ which can be many orders of magnitude greater than 1. Still, the system of Eqs. (21) is useful, because it can be solved analytically[69] in the general case for any lattice and for any value of ℓ. The analytical method of solving this system is described in Appendix E.

In what follows, it will be assumed that Eqs. (21) are solved and the LP unit cell additional charges

$$e(\boldsymbol{n})=e(n_1,n_2,n_3)$$

at points

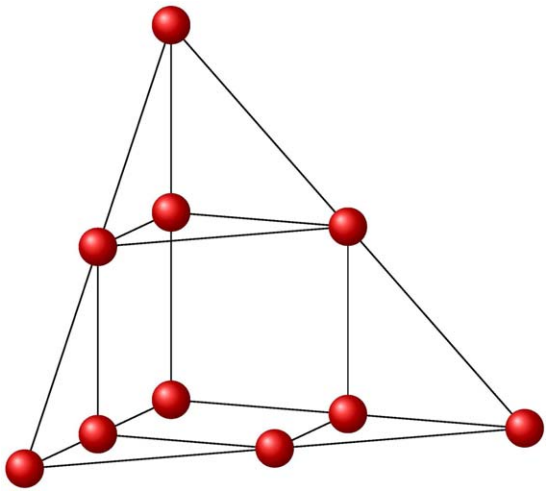

Figure 3. Tetrahedron of the unit cell additional charges for $\ell=2$.

$$\boldsymbol{d}(\boldsymbol{n})=\boldsymbol{d}(n_1,n_2,n_3)=n_1\boldsymbol{a}_1+n_2\boldsymbol{a}_2+n_3\boldsymbol{a}_3$$

are known.

The LP unit cell potential at point $\boldsymbol{r}$ is the sum

$$U(\boldsymbol{r})=U_1(\boldsymbol{r})+U_2(\boldsymbol{r}) \tag{22}$$

of the original unit cell potential

$$U_1(\boldsymbol{r})=\sum_{j=1}^{n_0}\frac{e_j}{|\boldsymbol{r}-\boldsymbol{\rho}_j|}$$

and the additional charges potential

$$U_2(\boldsymbol{r})=\sum_{\boldsymbol{n}\in T_\ell}\frac{e(\boldsymbol{n})}{|\boldsymbol{r}-\boldsymbol{R}_{\boldsymbol{n}}|}.$$

The system of LP unit cell additional charges has one important property, namely the sum of all additional charges is equal to zero

$$\sum_{\boldsymbol{n}\in T_\ell}e(\boldsymbol{n})=0. \tag{23}$$

Indeed, in the particular case $\boldsymbol{m}=0$, ($m_1=m_2=m_3=0$) Eq. (21) reads

$$\sum_{\boldsymbol{n}\in T_\ell}e(\boldsymbol{n})=-Q_0(0,0,0)$$

and the initial lattice unit cell is electrically neutral $Q_0(0,0,0)=0$.

Equation (23) is important because using this equation, one can prove that although the LP unit cell contains additional charges compared to the initial ones, the Ewald potential calculated with the LP unit cell coincides with the Ewald potential calculated with the initial lattice unit cell (Appendix E for proof). Besides, Eq. (23) makes it possible to generate a finite system of charges entirely outside the finite cluster to reproduce a perfect lattice potential in the cluster with any desirable precision. It will be shown the next section.

LP unit cell modifications. Apart from charges of the initial unit cell, the LP unit cell contains additional charges to annul the cell multipole moments. The LP unit cell additional charges occupy the lattice sites and form the tetrahedron. An example of this tetrahedron for the case of a maximal annulled moment $\ell=2$ is shown in Figure 3. Due to additional charges, the symmetry of an LP unit cell differs significantly from the symmetry of a conventional unit cell. However, the embedding potential will be calculated for the finite crystal obtained by the LP unit cell translations and not for one unit cell. These translations result in cancellation of all additional charges in the inner part of the finite crystal leaving only a comparatively thin layer of charges in the finite crystal border. Therefore, the effect of the unit cell symmetry difference on the embedding potential will be rather small. Nevertheless, it is desirable to minimize this difference, especially if some degenerate by the symmetry states should be considered.

It is possible to reduce the symmetry difference by accumulating the LP unit cell additional charges from eight tetrahedrons[70] instead from one, the additional charges in each tetrahedron annulling 1/8 of every multipole moment under consideration. There are two variants of these eight tetrahedrons dispositions, which will be demonstrated below in the case of simple cubic lattice.

The tetrahedron vertex at which three orthogonal edges of the tetrahedron meet will be referred to as a primary vertex. In the first variant, the primary vertex of each tetrahedron is put into the frame of reference origin and three orthogonal edges of each tetrahedron are directed along the Cartesian coordinate lines alternately in the positive or negative directions. The positions of the obtained additional charges in the LP unit cell in the case of maximal annulled moment $\ell=2$ are shown in Figure 4.

In the second variant, the primary vertex of the tetrahedron is put at the initial unit cell vertex and three orthogonal edges of the tetrahedron are directed along the initial unit cell edges so that the unit cell center will be inside the tetrahedron. This is done for each of the eight vertices of the initial unit cell. The positions of the additional charges in this LP unit cell are shown in Figure 5. It should be noted that in the second variant the more compact LP unit cell is obtained.

Some extra improvement can be achieved by moving the positions of the primary vertex.[70]

Far environment Coulomb potential. The far environment Coulomb (fec) potential is a point ion lattice potential involving all ions that do not belong to the cluster. It can be calculated as a potential of the perfect point ion lattice minus the potential produced by a finite number of charges corresponding to cluster atoms.

Let us first consider the perfect point ion lattice potential. Using an LP unit cell for a group and taking the lattice vector $\boldsymbol{R}_k$ for the group position vector $\boldsymbol{D}_k$, one will obtain an absolute (and fast) convergent series for the infinite point lattice potential

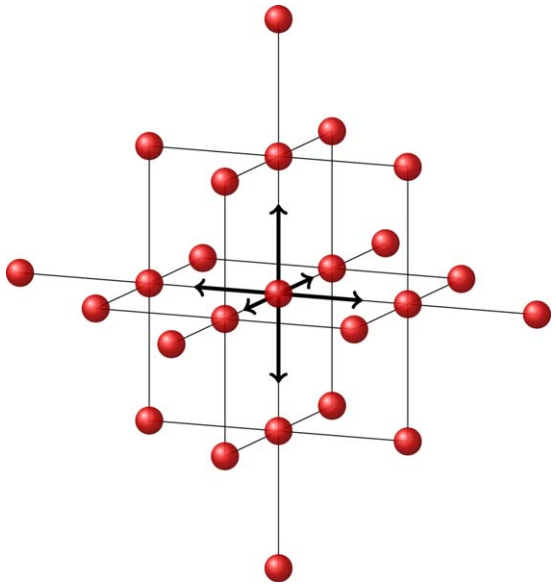

Figure 4. Eight tetrahedrons, variant 1.

$$V(\boldsymbol{r})=\sum_{k_1,k_2,k_3=-\infty}^{\infty} U(\boldsymbol{r}-\boldsymbol{R_k}), \qquad \boldsymbol{R}_k=k_1\boldsymbol{a}_1+k_2\boldsymbol{a}_2+k_3\boldsymbol{a}_3, \qquad (24)$$

where $U(\boldsymbol{r})$ is given by Eq. (22). Equation (24) describes the potential which coincides with the Ewald potential of the original lattice.

In what follows it will be assumed that the frame of reference origin is put at some point inside the cluster and the point lattice potential will be considered in some region around the frame of reference origin. Series (24) is absolutely convergent and its sum does not depend on the order of summation. Therefore, one can use the most convenient one. It is expedient to consider an integer N and to write series (24) as sum of the two series

$$V(\boldsymbol{r})=\sum_{\boldsymbol{k}\in\aleph} U(\boldsymbol{r}-\boldsymbol{R_k})+\sum_{\boldsymbol{k}\notin\aleph} U(\boldsymbol{r}-\boldsymbol{R_k}), \qquad (25)$$

where the summation region $\aleph$ contains all points $\boldsymbol{R_k}$ with

$$\boldsymbol{k}=(k_1,k_2,k_3), \qquad -N\le k_1,k_2,k_3\le N.$$

Because of the series absolute convergence, the second sum in (25) tends to zero when N tends to infinity. Hence, for any given precision ε one can find the finite value of N large enough to make the second sum absolute value smaller than ε. Therefore, within given precision one can take the potential

$$V^{(a)}(\boldsymbol{r})=\sum_{\boldsymbol{k}\in\aleph} U(\boldsymbol{r}-\boldsymbol{R_k}) \qquad (26)$$

as an approximation to the infinite lattice potential $V(\boldsymbol{r})$.

In Eq. (26), U is the sum (22) of U_1 and U_2. Therefore, the equation for the lattice potential can be written as

$$V(\boldsymbol{r})\approx V^{(a)}(\boldsymbol{r})=V_1^{(a)}(\boldsymbol{r})+V_2^{(a)}(\boldsymbol{r}),$$

where

$$V_1^{(a)}(\boldsymbol{r})=\sum_{\boldsymbol{k}\in\aleph} U_1(\boldsymbol{r}-\boldsymbol{R_k})=\sum_{\boldsymbol{k}\in\aleph}\sum_{j=1}^{\gamma}\frac{e_j}{|\boldsymbol{r}-\boldsymbol{\rho}_j-\boldsymbol{R_k}|}$$

and

$$V_2^{(a)}(\boldsymbol{r})=\sum_{\boldsymbol{k}\in\aleph} U_2(\boldsymbol{r}-\boldsymbol{R_k})=\sum_{\boldsymbol{k}\in\aleph}\sum_{\boldsymbol{n}\in T_\ell}\frac{e(\boldsymbol{n})}{|\boldsymbol{r}-\boldsymbol{R_n}-\boldsymbol{R_k}|}.$$

Both potentials $V_1^{(a)}$ and $V_2^{(a)}$ are due to a finite number of charges each. The potential $V_1^{(a)}$ is due to the finite lattice with integer number of initial unit cells. The correction for the infinite lattice is the potential $V_2^{(a)}$.

In the potential $V_2^{(a)}$, the sum $\boldsymbol{R_n}+\boldsymbol{R_k}$ is the lattice vector $\boldsymbol{R_i}$. By Υ, it will be denoted the region occupied by points i when $\boldsymbol{n}$ run over T_ℓ and $\boldsymbol{k}$ run over $\aleph$. The region Υ is larger than the region $\aleph$ and the same point $\boldsymbol{R_i}$ can be occupied by charges from different LP unit cells. The following equation is valid for the total charge $q(\boldsymbol{i})=q(i_1,i_2,i_3)$ accumulated at a point $\boldsymbol{R_i}$

$$q(\boldsymbol{i})=\sum_{\boldsymbol{k}\in\aleph}\sum_{\boldsymbol{n}\in T_\ell} e(\boldsymbol{n})\delta(\boldsymbol{k}+\boldsymbol{n}-\boldsymbol{i}).$$

With these notations on can write the equation for the potential $V_2^{(a)}(\boldsymbol{r})$ as

$$V_2^{(a)}(\boldsymbol{r})=\sum_{\boldsymbol{i}\in\Upsilon}\frac{q(\boldsymbol{i})}{|\boldsymbol{r}-\boldsymbol{R_i}|}. \qquad (27)$$

Formally, the sum over $\boldsymbol{i}$ in (27) is over all points belonging to Υ. However, because of (23) some charges $q(\boldsymbol{i})$ are equal to

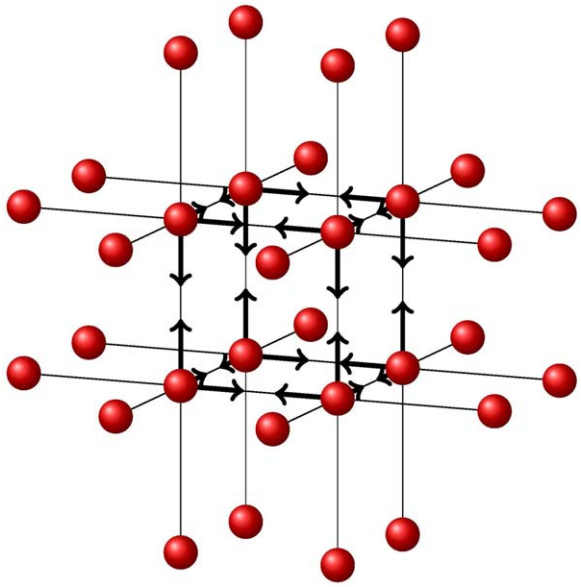

Figure 5. Eight tetrahedrons, variant 2.

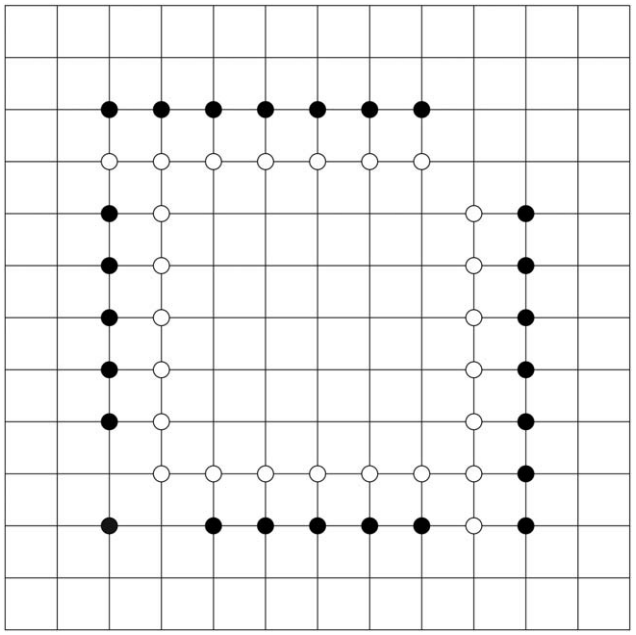

Figure 6. Nonzero additional charges in result of summation, 2-D case one triangle, $\ell=2$.

zero. Corresponding points $\boldsymbol{R_i}$ occupy the inner part of the region Υ. Indeed, consider point $\boldsymbol{R_i}$ with

$$-N+\ell \le i_1, i_2, i_3 < N, \tag{28}$$

where N determines the summation region $\aleph$ and ℓ is the maximal annulled moment. For any point $\boldsymbol{n} \in T_\ell$, one has

$$0 \le n_1, n_2, n_3 \le \ell.$$

Therefore, for the corresponding point $\boldsymbol{k}=\boldsymbol{i}-\boldsymbol{n}$, the following inequality is valid

$$-N \le k_1, k_2, k_3 \le N,$$

which means that point $\boldsymbol{k}$ belong to the summation region $\aleph$. Hence, for any point $\boldsymbol{n} \in T_\ell$ in the summation region $\aleph$, there exists point $\boldsymbol{k}$ for which

$$\boldsymbol{k}=\boldsymbol{i}-\boldsymbol{n}.$$

Consequently,

$$\sum_{\boldsymbol{k}\in\aleph} \delta(\boldsymbol{k}+\boldsymbol{n}-\boldsymbol{i})=1, \qquad \forall \boldsymbol{n} \in T_\ell$$

and

$$q(\boldsymbol{i})=\sum_{\boldsymbol{n}\in T_\ell}\sum_{\boldsymbol{k}\in\aleph} \delta(\boldsymbol{k}+\boldsymbol{n}-\boldsymbol{i})e(\boldsymbol{n})=\sum_{\boldsymbol{n}\in T_\ell} e(\boldsymbol{n})=0$$

due to (23). So the total charge $q(\boldsymbol{i})$ at inner points $\boldsymbol{i}$ (28) is equal to zero. The nonzero charge $q(\boldsymbol{i})$ can only be located in the border part of the region Υ. This border part will be denoted as Υ_b. The shape of this part is rather complicated. It is described in details in [69].

The results of the LP unit cell summation and additional charges cancellation in the inner region are shown below in the case of the 2-D lattice, where additional charges occupy triangle instead of the 3-D case tetrahedron. The square lattice is considered and the largest annulled multipole moment is chosen to be $\ell=2$. In Figure 6, the positions of the resulting nonzero additional charges are shown for the case of original LP unit cell, the white circles indicating the positive charges and black circles indicating the negative charges. The nonzero additional charges occupy only the border region but the square symmetry is lost. Similar results are shown in Figure 7 for the case of modified LP unit cell, variant 1. The square symmetry is restored but the size of the border layer is increased. The case of modified LP unit cell, variant 2, is shown in Figure 8. The square symmetry is restored and the size of the border region is less than that in the variant 1 of modified LP unit cell.

In the real finite crystal, the border region experiences various relaxation processes minimizing the potential outside the crystal. In the lattice potential calculations, the nonzero charges are added to the border region and minimized the electrostatic potential outside the crystal. Although the particular processes are different the total effect is the same. Therefore, one can consider calculation of the lattice potential with the help of an LP unit cell with additional charges as qualitative modeling the situation with the real finite crystal.

Considering the part of the perfect crystal near the frame of reference origin as a cluster, it is expedient to write the point ion lattice potential in somewhat different form. The part of the summation region $\aleph$, which corresponds to the cluster itself, will be denoted as $\aleph_c$ and the rest of the region $\aleph$, which corresponds to the cluster environment, will be denoted

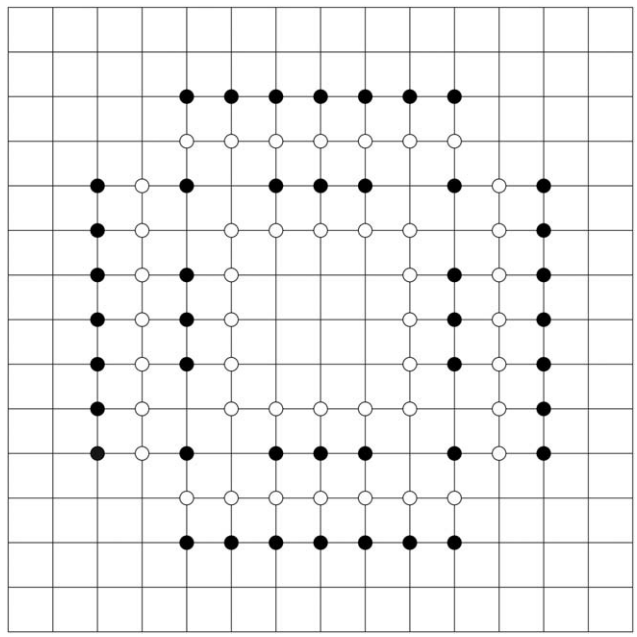

Figure 7. Nonzero additional charges in result of summation, 2-D case, four triangles, variant 1, $\ell=2$.

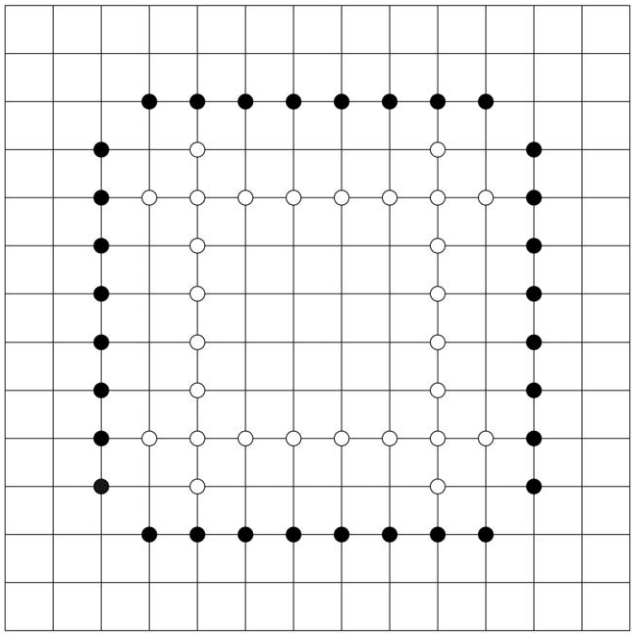

Figure 8. Nonzero additional charges in result of summation, 2-D case, four triangles, variant 2, $\ell=2$.

as $\aleph_e$. Then the point ion lattice potential can be written as sum

$$V(\boldsymbol{r})=V_c(\boldsymbol{r})+V_e(\boldsymbol{r}) \tag{29}$$

of the point ion lattice potential due to the cluster

$$V_c(\boldsymbol{r})=\sum_{\boldsymbol{k}\in\aleph_c} U_1(\boldsymbol{r}-\boldsymbol{R_k})=\sum_{\boldsymbol{k}\in\aleph_c}\sum_{j=1}^{n_0}\frac{e_j}{|\boldsymbol{r}-\boldsymbol{\rho}_j-\boldsymbol{R_k}|},$$

and the point ion lattice potential due to the cluster environment

$$V_e(\boldsymbol{r})=V_{e1}(\boldsymbol{r})+V_{e2}(\boldsymbol{r}),$$

where

$$V_{e1}(\boldsymbol{r})=\sum_{\boldsymbol{m}\in\aleph_e} U_1(\boldsymbol{r}-\boldsymbol{R_m})=\sum_{\boldsymbol{k}\in\aleph_e}\sum_{j=1}^{n_0}\frac{e_j}{|\boldsymbol{r}-\boldsymbol{\rho}_j-\boldsymbol{R_k}|}$$

is the point ion finite lattice potential and

$$V_{e2}(\boldsymbol{r})=\sum_{\boldsymbol{i}\in\Upsilon_b}\frac{q(\boldsymbol{i})}{|\boldsymbol{r}-\boldsymbol{R_i}|}$$

is the correction for the infinite lattice. This is potential $V_2^{(a)}(\boldsymbol{r})$ but contrary to the Eq. (27), the summation here is over only border part of the region Υ containing nonzero charges $q(\boldsymbol{i})$.

All charges producing potential $V_e(\boldsymbol{r})$ are situated outside the cluster. Hence, $V_e(\boldsymbol{r})$ is the potential due to the cluster far environment. Therefore, it can be considered as a contribution to the embedding potential. It is expedient to refer to potential $V_e(\boldsymbol{r})$ as the fec embedding potential

$$V_{\text{fec}}(\boldsymbol{r})\equiv V_e(\boldsymbol{r})=\sum_{\boldsymbol{k}\in\aleph_e}\sum_{j=1}^{n_0}\frac{e_j}{|\boldsymbol{r}-\boldsymbol{\rho}_j-\boldsymbol{R_k}|}+\sum_{\boldsymbol{i}\in\Upsilon_b}\frac{q(\boldsymbol{i})}{|\boldsymbol{r}-\boldsymbol{R_i}|}. \tag{30}$$

Note that potential $V_{\text{fec}}(\boldsymbol{r})$ is determined by charges outside the cluster, and therefore, the same potential $V_{\text{fec}}(\boldsymbol{r})$ can be used in the calculations of both a perfect crystal and a crystal with defect, providing the defect is local.

Near environment Coulomb potential. The cluster near environment consists of border atoms orbitals directed outward the cluster. The near environment Coulomb (nec) potential is the long-range part of the near environment potential and the potential of a point charges system will be taken to represent it. Each charge corresponds to one border atom. The position of this charge is not really important because the potential difference resulting from different positions of the point charges will be taken into account together with the short-range part of the embedding potential. Therefore, the border atom nucleus position has been selected for the point charge position. The value of this charge can be calculated as follows. All border atoms of the cluster are of the same type (Types 1 or 2). Each border atom has the same number m (m_1 or m_2) of bonds attached to it but different border atoms can have a different number of bonds directed outward the cluster. For jth border atom, the number of bonds directed inward the cluster is denoted as $\mu_j^{'}$ and the number of bonds directed outward the cluster is denoted as $\mu_j^{''}$, where

$$\mu_j^{'}+\mu_j^{''}=m.$$

Each bond contributes charge ω [ω_1 or ω_2, see Eq. (12)] to the border atom (all bonds are equivalent). So the total charge $q_j^{(\text{nec})}$ due to all outward bonds of the border ion j is

$$q_j^{(\text{nec})}=\omega\mu_j^{''}.$$

Consequently, the nec embedding potential is

$$V_{\text{nec}}(\boldsymbol{r})=\sum_{j=1}^{n_b}\frac{q_j^{(\text{nec})}}{|\boldsymbol{r}-\boldsymbol{R}_j|}. \tag{31}$$

The sum is over all border atoms. The number n_b of border atoms is comparatively small, and this sum can be easily calculated.

Short-range embedding

The Coulomb embedding potential is the long-range part of the embedding potential. The difference between a total embedding potential and its long-range part can be considered as the short-range part of the embedding potential. Several different methods were proposed to generate the short-range part of an embedding potential. For example, the Adams–Gilbert equations (11) were used for the self-consistent calculations of several overlapping electron groups.[54,58,71] The particular form of potential depends on the localization functional employed. Two particular functionals,[58] one of which

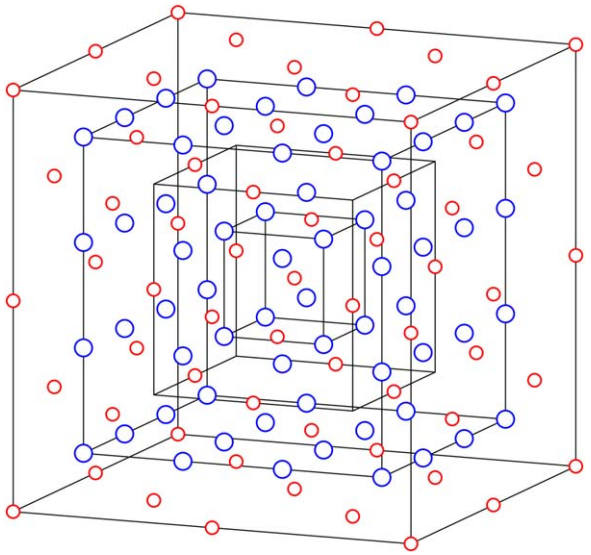

Figure 9. Cluster $O_{64}Zr_{63}^{(ps)}$.

maximizes the Mullikens[72] net atomic population in the selected region[54,55,73,74] and the other[53,54] use a Fock operator for the localizing operator $\hat{A}$, produce similar results.

In the AIMP approach,[19] the approximate one-electron orbitals are used for the cluster environment, and the embedding potential is derived using the corresponding coulomb-exchange operators.

In [75], a number of simple trial potentials with parameters are selected and parameters are defined with the trial and error method to reproduce a number of specifically chosen properties of the cluster in a crystal. One-center and multicenter potentials were used.

The approach described below is based on the cluster in crystal notion and on the division of the crystal into the cluster and cluster environment discussed in "Ion-covalent crystal" section. Using the finite crystal molecular orbitals and applying a localization procedure to them, one can calculate the noncanonical molecular orbitals of the crystal, which can be considered as molecular orbitals of a cluster in a crystal and with their help one can generate an embedding potential. In this approach, both the occupied and virtual states of a cluster in a crystal should be used.

As in previous sections, the ion-covalent crystals are considered here. To avoid the unnecessary complications, the valence electrons only approximation is adopted. It is assumed that the crystal contains atoms of only two types, one anion and one cation, and all the nearest anion–cation bonds are equivalent. The cubic phase of ZrO_2 crystal is the convenient system with all described above properties. In this crystal, each oxygen contributes six electrons and each zirconium contributes four electrons to the valence electrons system. All other electrons of oxygen and zirconium are taken into account with the help of ECP. As a particular finite crystal, the cluster shown in Figure 9 was chosen. This cluster is under the influence of ZrO_2 Coulomb embedding potential. It contains 64 oxygen and 13 zirconium ions in its inner part and only zirconium ions at its border. There are 30 zirconium ions situated at the cube faces. Four out of eight bonds connected with each of these zirconiums belong to the cluster and the other four belong to the cluster environment. Besides, there are 12 zirconiums at the cube edges with two bonds belonging to the cluster and six bonds belonging to the cluster environment. Finally, there are 8 zirconiums at the cube vertices with one bond belonging to the cluster and seven bonds belonging to the cluster environment. Therefore, this cluster can be designated as $O_{64}Zr_{13}\,Zr_{30/2}Zr_{12/4}Zr_{8/8}$. We will use short notation $O_{64}Zr_{63}^{(ps)}$ for this cluster when possible.

Three different small clusters will be considered. Cluster $OZr_{4/8}$ containing four bonds with cations at the border is shown in Figure 10. Containing eight bonds cluster $ZrO_{8/4}$ with anions at the border is shown in Figure 11. Cluster $O_8Zr_1Zr_{12/4}$ containing 32 bonds with one cation at its center and 12 cations at the border is shown in Figure 12.

Assume that the finite crystal is calculated in the MO–LCAO approximation and all molecular orbitals Ψ_j (occupied and virtual) and corresponding one-electron energies E_j (ionization potentials) are known. The atomic basis functions are denoted as $\chi_{ak}(\boldsymbol{r})$ where $a=1,\cdots,N_{at}$ is the atom index and $k=1,\cdots,$ v_a is the basis function of the atom a index. The number of basis functions for the atom a is denoted as v_a. The total number of finite crystal atomic basis functions is N_0. The total number of finite crystal canonical orbitals is equal to the total number of atomic basis functions. The number of finite crystal occupied molecular orbitals is N_{occ}, so the number of finite crystal virtual molecular orbitals is $N_{virt}=N_0-N_{occ}$. The finite crystal molecular orbitals Ψ_j are canonical orbitals spread over the whole volume of the crystal. In what follows, noncanonical orbitals localized in a part of the crystal will be used, and, in particular, orbitals localized in the region of one and only one pair of the nearest anion and cation will be used. These orbitals are referred to as bond orbitals. It is assumed that transformation to the crystal noncanonical localized orbitals can be made in which all occupied orbitals are the bond orbitals. The cluster is a closed part of the finite crystal which contains an

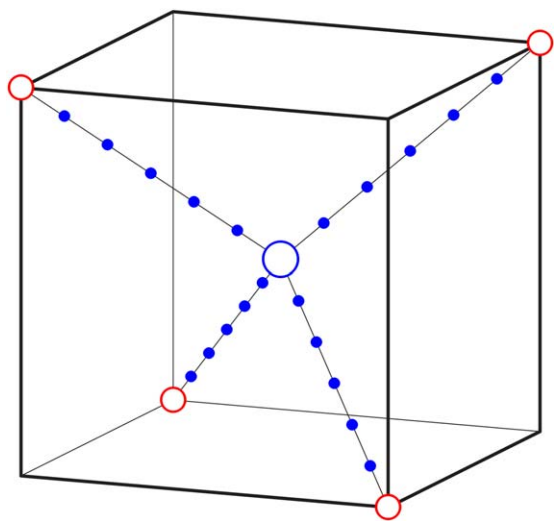

Figure 10. Cluster $OZr_{4/8}$ and positions of auxiliary basis functions.

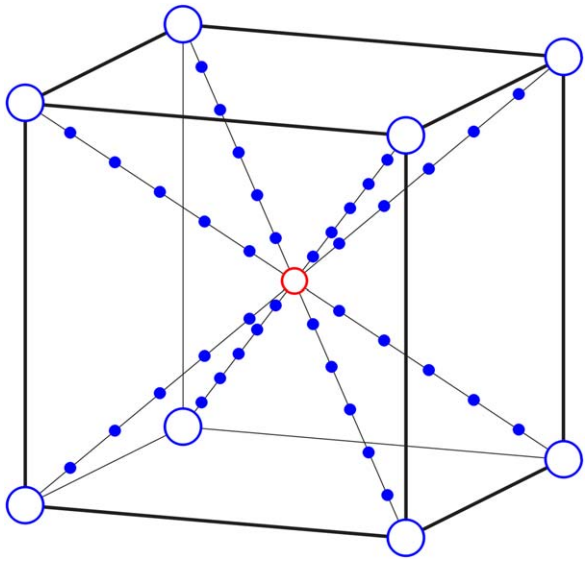

Figure 11. Cluster $ZrO_{8/4}$ and position of auxiliary basis functions.

integer number n_{occ} of bond orbitals; and these are the only occupied orbitals of the cluster.

Two different localization procedures will be used to calculate the cluster in crystal orbitals: one for occupied states and the other for virtual states. In the case of occupied states, the well localized auxiliary 1s Gaussian functions

$$g(\boldsymbol{r})=\left(\frac{2\alpha}{\pi}\right)^{3/4}\exp(-\alpha r^2)$$

with the same sufficiently large parameter α are used. For each bond of the crystal, a set of $n_g \sim 10, 20$ functions

$$g_{nj}(\boldsymbol{r})=g(\boldsymbol{r}-\boldsymbol{R}_{nj}), \qquad j=1,\cdots,n_g \tag{32}$$

at equidistant points $\boldsymbol{R}_{nj}$ along the line connecting the corresponding anion and cation of the nth bond is generated. Positions of auxiliary functions in clusters $OZr_{4/8}$ and $ZrO_{8/4}$ are shown by dots in Figures 10 and 11. Projector onto the set of nth bond auxiliary functions is

$$\hat{P}_{ng}=\sum_{j,k=1}^{n_g}|g_{nj}\rangle\{G^{-1}\}_{nj,nk}\langle g_{nk}|, \tag{33}$$

where $G_{nj,nk}$ is the overlap matrix of g_{nj} and g_{nk} auxiliary functions. With the help of crystal occupied canonical orbitals Ψ_j the matrix of the projector $\hat{P}_{ng}$ can be calculated, and its eigenvectors and eigenvalues can be found

$$\sum_{j=1}^{N_{occ}}\langle\Psi_k|\hat{P}_{ng}|\Psi_j\rangle D_{\ell j}=\mu_\ell D_{\ell k}, \qquad k=1,\ldots,N_{\rm occ}. \tag{34}$$

The eigenvector corresponding to the largest eigenvalue μ_i provides coefficients $C_{nj}^{(bd)}=D_{ij}$ for bond orbital $\Phi_n^{(bd)}(\boldsymbol{r})$ expansion over occupied canonical orbitals

$$\Phi_n^{(bd)}(\boldsymbol{r})=\sum_{j=1}^{N_{occ}}C_{nj}^{(bd)}\Psi_j(\boldsymbol{r}).$$

This bond orbital is normalized to 1 and is the linear combination of all atomic basis functions χ_{aj} of the crystal.

At the same time, a bond basis can be made for each bond as a union of atomic bases of corresponding atoms; and the projector

$$\hat{P}_n^{(bd)}=\sum_{\ell m}^{(a,b)}\sum_{j=1}^{\nu_\ell}\sum_{k=1}^{\nu_m}|\chi_{\ell j}\rangle\{S_{bd}^{-1}\}_{\ell j,mk}\langle\chi_{mk}|$$

onto the nth bond basis can be calculated. Here, sum over ℓ and m is over atoms a and b of the bond and S_{bd} is the overlap matrix of bond basis functions. With the help of this projector, the bond orbital $\varphi_n^{(bd)}(\boldsymbol{r})$ in bond basis can be obtained

$$\varphi_n^{(bd)}(\boldsymbol{r})=\hat{P}_n^{(bd)}\Phi_n^{(bd)}(\boldsymbol{r}).$$

To estimate the quality of bond orbital $\varphi_n^{(bd)}(\boldsymbol{r})$ localization the norm square was calculated for each bond. For any bond in the $O_{64}Zr_{63}^{(ps)}$ cluster, the deviation of the norm square from 1 was found to be less than 0.03. So 97% of the bond electron density is in the bond region.

The $O_{64}Zr_{63}^{(ps)}$ cluster contains 256 bonds and 104 of them are inner bonds (not connected with border Zr). To check whether occupied bond orbitals can be considered as equivalent, all bond orbitals in bond basis $\varphi_n^{(bd)}(\boldsymbol{r})$ were normalized to 1 and rotated to the same frame of reference. All overlap integrals between rotated bond orbitals were calculated. The maximum deviation from 1 of the overlap integral for inner bonds was found to be 0.00013, and for all bonds, including bonds with border Zr, the maximum deviation from 1 was found to be 0.0041. Thus, the inner bond orbitals can be considered as equivalent and bond orbitals with border Zr are close to them.

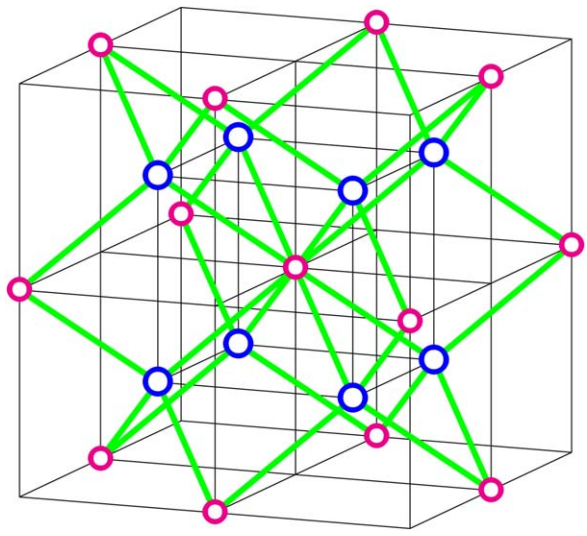

Figure 12. Cluster $O_8Zr_1Zr_{12/4}$ with the diatomic bonds.

The employment of the intermediate basis set (32) in the bond orbitals $\varphi_n^{(bd)}(\boldsymbol{r})$ calculations is essential. For example, when the bond orbitals in bond basis $\varphi_n^{(bd)}(\boldsymbol{r})$ were calculated from the occupied canonical orbitals Ψ_j with the projector $\hat{P}_n^{(bd)}$ used in the Eq. (34), the ratio between the second largest and the largest eigenvalues of the projector $\hat{P}_n^{(bd)}$ was found to be 0.99. In this case, arguments in favor of the function with the largest eigenvalue comparing with the function with the second largest eigenvalue are rather weak. In the case of the two steps procedure (the first step with the projector $\hat{P}_{ng}$ and the second step with the projector $\hat{P}_n^{(bd)}$) the corresponding ratio (for eigenvalues of the projector $\hat{P}_{ng}$) was found to be 0.02. In this case, the orbital corresponding to the largest eigenvalue is undoubtedly the most localized one.

Using the described localization procedure, the bond orbitals $\Phi_n^{(bd)}(\boldsymbol{r})$ in the finite crystal total basis can be calculated for all bonds, $n=1,\ldots,N_{\mathrm{occ}}$. It is assumed that the orbitals $\Phi_n^{(bd)}(\boldsymbol{r})$ are numerated so that the orbitals corresponding to the bonds belonging to the cluster are the first on the list. The orbitals $\Phi_n^{(bd)}(\boldsymbol{r})$, $n=1,\ldots,n_{\mathrm{occ}}$ localized on bonds belonging to the cluster can be considered as occupied orbitals of the cluster in the crystal. However, these are directed nonorthogonal orbitals, and therefore, they are noncanonical orbitals of the cluster. Canonical orbitals are linear combinations of directed orbitals, and coefficients in these linear combinations can be found with the help of the Fock operator for the finite crystal.

With operator spectral decomposition, the Fock operator of finite crystal can be written as

$$\hat{F}=\sum_{j=1}^{N_0}|\Psi_j\rangle\, E_j\langle\Psi_j|,$$

this operator can be considered as the sum

$$\hat{F}=\hat{F}^{(\mathrm{occ})}+\hat{F}^{(\mathrm{virt})}$$

of

$$\hat{F}^{(\mathrm{occ})}=\sum_{j=1}^{N_{\mathrm{occ}}}|\Psi_j\rangle\, E_j\langle\Psi_j| \tag{35}$$

the Fock operator for occupied states and

$$\hat{F}^{(\mathrm{virt})}=\sum_{j=N_{\mathrm{occ}}+1}^{N_0}|\Psi_j\rangle\, E_j\langle\Psi_j| \tag{36}$$

the Fock operator for virtual states.

Using the Fock operator for occupied states (35), one can generate canonical occupied orbitals for the cluster in the crystal and calculate corresponding energies. To do this, the matrix of the operator $\hat{F}^{(\mathrm{occ})}$ can be calculated with noncanonical orbitals $\Phi_n^{(bd)}(\boldsymbol{r})\, n=1,\ldots,n_{\mathrm{occ}}$, and the corresponding eigenvectors and eigenvalues problem can be solved

$$\sum_{m=1}^{n_{\mathrm{occ}}}\langle\Phi_n^{(bd)}|\hat{F}^{(\mathrm{occ})}|\Phi_m^{(bd)}\rangle C_{nm}=E_n^{(cl)}\sum_{m=1}^{n_{\mathrm{occ}}}\langle\Phi_n^{(bd)}|\Phi_m^{(bd)}\rangle C_{nm},\quad n=1,\ldots,n_{\mathrm{occ}}. \tag{37}$$

The orthonormal noncanonical orbitals of the finite crystal

$$\Phi_n^{(cl)}(\boldsymbol{r})=\sum_{m=1}^{n_{\mathrm{occ}}}C_{nm}\Phi_m^{(bd)}(\boldsymbol{r})\qquad n=1,\ldots,n_{\mathrm{occ}} \tag{38}$$

are localized in the cluster volume and span the same functional space as bond orbitals $\Phi_n^{(bd)}$. Therefore, orbitals $\Phi_n^{(cl)}(\boldsymbol{r})$ and energies $E_n^{(cl)}$ will be considered as occupied canonical orbitals and energies of the cluster in the crystal.

The canonical occupied orbitals $\Phi_n^{(cl)}(\boldsymbol{r})$ are obtained in the atomic basis of the finite crystal. However, for applications, it is necessary to have cluster orbitals in the cluster basis. It is expedient to obtain these orbitals with the help of the projector

$$\hat{P}^{(cl)}=\sum_{a,b}^{(cl)}\sum_{j=1}^{\nu_a}\sum_{k=1}^{\nu_b}|\chi_{aj}\rangle\left\{S_{cl}^{-1}\right\}_{aj,bk}\langle\chi_{bk}| \tag{39}$$

onto the cluster basis. Here, the sum is over all cluster basis functions and S_{cl} is the corresponding overlap matrix. Functions

$$f_n(\boldsymbol{r})=\hat{P}^{(cl)}\Phi_n^{(cl)}(\boldsymbol{r})\qquad n=1,\ldots,n_{\mathrm{occ}}$$

are in the cluster basis, but they are, in general, not normalized to 1 and not orthogonal to each other. However, the overlap matrix

$$S_{nm}=\langle f_n|f_m\rangle,\qquad n,m=1,\ldots,n_{\mathrm{occ}}$$

is usually close to the unit matrix. Using the Lowdin equation for symmetrical orthonormalization

$$\psi_n^{(cl)}(\boldsymbol{r})=\sum_{m=1}^{n_{\mathrm{occ}}}\left\{S^{-1/2}\right\}_{nm}f_m(\boldsymbol{r}),\qquad n=1,\ldots,n_{\mathrm{occ}} \tag{40}$$

the orthonormal orbitals $\psi_n^{(cl)}(\boldsymbol{r})$ in the cluster basis can be obtained.

The orbitals $\psi_n^{(cl)}(\boldsymbol{r})$ and energies $E_n^{(cl)}$ will be considered as occupied canonical molecular orbitals and one-electron energies of the cluster in the ion-covalent crystal.

Note, that although no approximations were used in orbitals $\Phi_n^{(cl)}(\boldsymbol{r})$ calculations from the crystal molecular orbitals $\Psi_j(\boldsymbol{r})$, the orbitals $\psi_n^{(cl)}(\boldsymbol{r})$ are approximate due to the projection from the crystal basis to the cluster basis.

A somewhat different method will be used to calculate a cluster in crystal virtual orbitals. Cluster virtual orbitals should be calculated as linear combinations of finite crystal virtual orbitals. It is essential that cluster virtual orbitals are spread over the whole volume of the cluster and not only over its inner part as occupied cluster orbitals. Therefore, instead of projector (33) onto the auxiliary functions, the projector onto the cluster basis (39) should be used. Hence, one arrives at the following equation

$$\sum_{j=1}^{N_{\text{virt}}} \langle \Psi_{k+N_{\text{occ}}} | \hat{P}^{(cl)} | \Psi_{j+N_{\text{occ}}} \rangle D_{\ell j} = \mu_\ell D_{\ell k}, \qquad k=1,\ldots,N_{\text{virt}} \quad (41)$$

to produce virtual orbitals localized in the cluster. In this equation, N_{virt} is the number of virtual orbitals in the finite crystal. The number n_0 of cluster atomic basis functions is

$$n_0 = \sum_a^{(cl)} v_a,$$

where sum is over atoms of the cluster. Consequently, the number of virtual orbitals in the cluster is $n_{\text{virt}} = n_0 - n_{\text{occ}}$. From the Eq. (41), n_{virt} localized in the cluster virtual orbitals can be obtained. Assume that eigenvectors $D_{\ell j}$ and eigenvalues μ_ℓ are arranged in the decreasing μ_ℓ value. Then functions

$$\Phi_n^{(v)}(\boldsymbol{r}) = \sum_{j=1}^{N_{\text{virt}}} D_{nj} \Psi_{j+N_{\text{occ}}}(\boldsymbol{r}), \qquad n=1,\ldots,n_{\text{virt}}$$

are virtual (noncanonical) orbitals of finite crystal (similar to $\Phi_n^{(bd)}(\boldsymbol{r})$ in the case of occupied states) localized in the cluster. These functions are considered as noncanonical virtual orbitals of the cluster in the crystal. They are orthonormal as eigenfunction of one operator. To find the corresponding canonical virtual orbitals, the Fock operator (36) for virtual states can be used, and the following equation can be used

$$\sum_{m=1}^{n_{\text{virt}}} \langle \Phi_n^{(v)} | \hat{F}^{(\text{virt})} | \Phi_m^{(v)} \rangle C_{nm} = E_{n+n_{\text{occ}}}^{(cl)} C_{nn}, \qquad n=1,\ldots,n_{\text{virt}}. \quad (42)$$

This equation eigenfunctions

$$\Phi_{n+n_{\text{occ}}}^{(cl)}(\boldsymbol{r}) = \sum_{m=1}^{n_{\text{virt}}} C_{nm} \Phi_m^{(v)}(\boldsymbol{r}), \qquad n=1,\ldots,n_{\text{virt}} \quad (43)$$

are cluster canonical virtual orbitals in the total atomic basis of the crystal and $E_{n+n_{\text{occ}}}^{(cl)}$ are the cluster in crystal virtual one-electron energies.

The obtained cluster virtual orbitals (43) and occupied orbitals (38) in the crystal atomic basis are orthogonal to each other, because the cluster virtual orbital is a linear combination of crystal virtual orbitals; the cluster occupied orbital is a linear combination of crystal occupied orbitals; and the crystal occupied and virtual orbitals in the crystal atomic basis are orthogonal to each other.

When considering cluster virtual orbitals in the cluster atomic basis calculations, it is necessary to take into account that both in the case of the cluster basis and in the case of the crystal basis, all virtual orbitals should be orthogonal to occupied orbitals. Therefore, a projector onto the whole cluster basis is not appropriate. It is necessary instead to take a projector onto the orthogonal complement to the cluster occupied orbitals. In this case, each cluster virtual orbitals will be a linear combination of functions orthogonal to occupied orbitals.

The projector onto the orthogonal complement can be written as the difference

$$\hat{P}^{(\text{cmpl})} = \hat{P}^{(cl)} - \hat{P}^{(\text{occ})} \quad (44)$$

between projector (39) onto the cluster basis and projector onto the cluster orthonormal occupied states (40)

$$\hat{P}^{(\text{occ})} = \sum_{n=1}^{n_{\text{occ}}} |\psi_n^{(cl)}\rangle \langle \psi_n^{(cl)}|. \quad (45)$$

Then projections of cluster virtual orbitals in the crystal atomic basis

$$f_n(\boldsymbol{r}) = \hat{P}^{(\text{cmpl})} \Phi_{n+n_{\text{occ}}}^{(cl)}(\boldsymbol{r}) \qquad n=1,\ldots,n_{\text{virt}}$$

are functions in the cluster basis which are orthogonal to the occupied orbitals of cluster. However, these functions overlap matrix

$$S_{nm} = \langle f_n | f_m \rangle, \qquad n,m=1,\ldots,n_{\text{virt}}$$

usually deviates from the unit matrix. Using Lowdin equation for the symmetrical orthonormalization

$$\psi_{n+n_{\text{occ}}}^{(cl)}(\boldsymbol{r}) = \sum_{m=1}^{n_{\text{virt}}} \left\{ S^{-1/2} \right\}_{nm} f_m(\boldsymbol{r}), \qquad n=1,\ldots,n_{\text{virt}} \quad (46)$$

the orbitals $\psi_{n+n_{\text{occ}}}^{(cl)}(\boldsymbol{r})$ can be obtained which are orthonormal and orthogonal to the cluster occupied orbitals.

The orbitals $\psi_{n+n_{\text{occ}}}^{(cl)}(\boldsymbol{r})$ and energies $E_{n+n_{\text{occ}}}^{(cl)}$ with $n=1,\ldots,n_{\text{virt}}$ will be considered as virtual canonical molecular orbitals and one-electron energies of a cluster in an ion-covalent crystal.

The cluster in crystal orbitals $\psi_n^{(cl)}(\boldsymbol{r})$ and energies $E_n^{(cl)}$ for $n=1,\ldots,n_0$ were calculated as it was described above for cluster $O_{64}Zr_{63}^{(ps)}$ as a finite crystal and for several small clusters in it. In Figure 13, the $O_{64}Zr_{63}^{(ps)}$ cluster density of states is shown together with occupied and lowest virtual energy levels for $OZr_{4/8}$, $ZrO_{8/4}$, and $O_8Zr_1Zr_{12/4}$ clusters calculated with the help of Eqs. (37) and (42). The obtained energy levels disposition can be considered as satisfactory.

Using the obtained occupied and virtual cluster orbitals $\psi_n^{(cl)}(\boldsymbol{r})$ [Eqs. (40) and (46)] and energies $E_n^{(cl)}$ [Eqs. (37) and (42)], a short-range part of the embedding potential can be generated. The problem is: given the orbitals $\psi_n^{(cl)}(\boldsymbol{r})$ and energies $E_n^{(cl)}$ for occupied and virtual stated of the cluster, generate the embedding potential so that the self-consistent field calculations of the cluster in the generated embedding potential reproduce given orbitals and energies. This problem has an exact solution.

To generate the embedding potential from given orbitals and energy levels, the spectral decomposition of the Fock operator for the cluster is used

$$\hat{F}_{cl} = \sum_{n=1}^{n_0} |\psi_n^{(cl)}\rangle E_n^{(cl)} \langle \psi_n^{(cl)}|. \quad (47)$$

At the same time, the Fock operator for the cluster in the embedding potential is

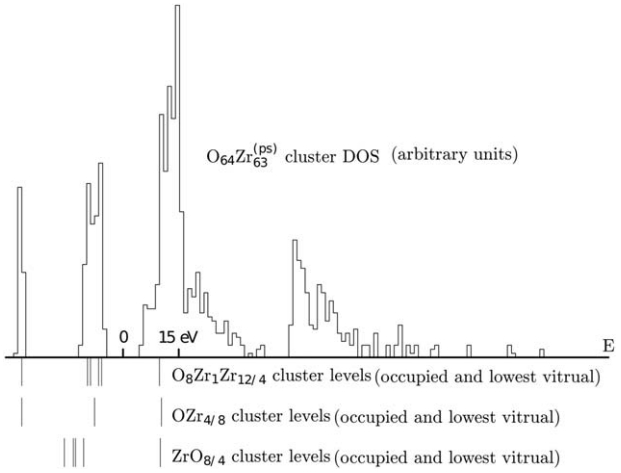

Figure 13. Density of states of the cluster $O_{64}Zr_{63}^{(ps)}$ and energy levels of clusters $OZr_{4/8}$, $O_8Zr_1Zr_{12/4}$, and $ZrO_{8/4}$.

$$\hat{F}_{cl}=\hat{T}+\hat{V}_0+\hat{U}+\hat{V}_{\text{fec}}+\hat{V}_{\text{nec}}+\hat{V}_{sr}. \tag{48}$$

where $\hat{T}$ is the kinetic energy operator, V_0 is the nuclear attraction and the external field potential (if any), and $\hat{U}$ is the Coulomb-exchange operator

$$\hat{U}f(\boldsymbol{r})=\int\frac{\rho(\boldsymbol{r}'|\boldsymbol{r}')}{|\boldsymbol{r}-\boldsymbol{r}'|}d\boldsymbol{r}'f(\boldsymbol{r})-\frac{1}{2}\int\frac{\rho(\boldsymbol{r}|\boldsymbol{r}')}{|\boldsymbol{r}-\boldsymbol{r}'|}f(\boldsymbol{r}')d\boldsymbol{r}'$$

with the cluster density matrix

$$\rho(\boldsymbol{r}|\boldsymbol{r}')=2\sum_{n=1}^{n_{\text{occ}}}\psi_n^{(cl)}(\boldsymbol{r})\psi_n^{(cl)^*}(\boldsymbol{r}')$$

calculated with cluster occupied orbitals $\psi_n^{(cl)}(\boldsymbol{r})$, V_{fec} is the fec potential (30), V_{nec} is the nec potential (31), and $\hat{V}_{sr}$ is the short-range embedding potential.

Combining Eqs. (47) and (48), the following equation for the short-range embedding potential can be obtained

$$\hat{V}_{sr}=\sum_{n=1}^{n_0}|\psi_n^{(cl)}>E_n<\psi_n^{(cl)}|-\hat{T}-V_0-\hat{U}-V_{\text{fec}}-V_{\text{nec}}. \tag{49}$$

All terms in the right-hand side of the Eq. (49) are known; so (49) is the equation for the exact short-range embedding potential.

If the MO-LCAO approximation is used, then all operators are in the matrix representation. From Eq. (49), the short-range embedding potential matrix $\{V_{sr}\}_{jk}$ can be calculated. This matrix is for the particular cluster with the particular atomic basis used in calculations, and as is it can be used only for the cluster considered. However, the short-range embedding potential obtained for one cluster can be used in another cluster calculations if the border regions of both clusters are the same, and the difference is only in the inner parts of clusters. For example, one cluster can be a cluster of the perfect crystal and another cluster can have defects in its inner part, impurity atom, vacancy, or different geometry of cluster atoms. In this case, the perfect crystal short-range embedding potential matrix $\{V_{sr}\}_{jk}$ can be used to generate the corresponding operator

$$\hat{V}_{sr}=\sum_{jk}|\chi_j\rangle\sum_{\ell m}\{S^{-1}\}_{j\ell}\{V_{sr}\}_{\ell m}\{S^{-1}\}_{mk}\langle\chi_k|, \tag{50}$$

where χ_j are the perfect cluster atomic basis functions and S is the basis overlap matrix. It is evident that operator (50) matrix with χ_j basis functions is $\{V_{sr}\}_{jk}$. However, Eq. (50) can be used for the short-range embedding potential matrix calculations with another basis. Therefore, operator (50) can be used for the cluster with defect calculations.

The self-consistent field calculations were performed for clusters $OZr_{4/8}$, $O_8Zr_1Zr_{12/4}$, and $ZrO_{8/4}$ in the Coulomb embedding potential. In Table 1, the lowest energy level, the highest occupied energy level, and the lowest virtual energy level are shown for clusters $OZr_{4/8}$ and $O_8Zr_1Zr_{12/4}$ with Zr atoms at the border obtained as eigenvalues of Eqs. (37) and (42) together with the corresponding energy levels of clusters in the Coulomb embedding potential. From this table, one can see that the occupied energy levels are in good agreement and the agreement for $O_8Zr_1Zr_{12/4}$ cluster is better. However, the difference between the virtual levels is about 5 eV. At the same time, there was no agreement at all in the case of $ZrO_{8/4}$ cluster with oxygen at the border in the Coulomb embedding potential, and even the self-consistent field calculations convergence was problematic. Calculations of all three clusters with the added short-range embedding potential reproduced (as it should be) all occupied and virtual levels. These results indicate that the short-range embedding potential is important, and it is really the short-range potential; so its influence depends on the electron density at the border atoms. For occupied states in clusters $OZr_{4/8}$ and $O_8Zr_1Zr_{12/4}$, the electron density on border atoms is comparatively small, whereas for virtual states in these clusters, the border density is larger and in the $ZrO_{8/4}$ cluster almost all electron density is localized on border atoms both in the occupied and lowest virtual states.

The embedding potential can be used not only for the clusters with defect electronic structure calculations but also for the ion-covalent crystals band structure calculations. In the band structure calculations using atomic basis functions χ_{aj}, the matrix elements with atomic basis functions are used,

Table 1. Energy levels (au) of $OZr_{4/8}$ and $O_8Zr_1Zr_{12/4}$ clusters.

		$OZr_{4/8}$		$O_8Zr_1Zr_{12/4}$	
	n	E_n	$E_n^{'}$	E_n	$E_n^{'}$
1s	1	−0.996	−1.010	−1.027	−1.029
HOMO	n_{occ}	−0.282	−0.296	−0.218	−0.219
LUMO	$n_{\text{occ}}+1$	0.370	0.233	0.361	0.205

Lowest energy level (1s), highest occupied level (HOMO), and lowest virtual level (LUMO) are shown for both clusters. Here, $E_n=E_n^{(cl)}$ are eigenvalues of (37)) for occupied states and $E_n=E_{n_{\text{occ}}+1}^{(cl)}$ are eigenvalues of (42)) for virtual state. $E_n^{'}$ are the corresponding energy levels calculated for cluster in the Coulomb embedding potential

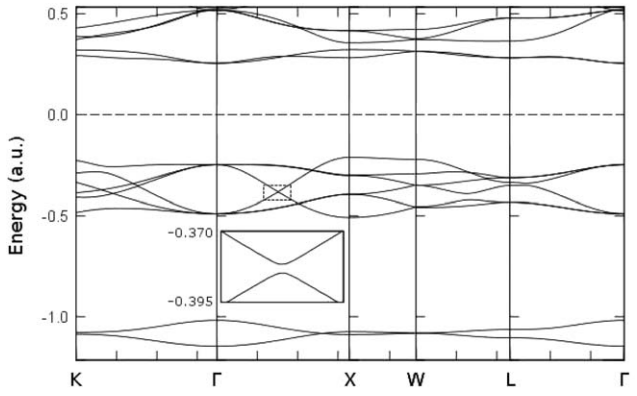

Figure 14. Band structure of cubic ZrO_2.

namely, the matrix elements of the crystal potential $\hat{V}^{(cr)}$ calculated with atomic basis functions χ_{aj} and χ_{bk} where the atom a is in one unit cell and the atom b is in the neighboring unit cell. However, the potential $\hat{V}^{(cl)}$ of the cluster in the embedding potential is an approximation to the crystal potential. Therefore, the approximation can be used

$$\langle\chi_{aj}|\hat{V}^{(cr)}|\chi_{bk}\rangle \approx \langle\chi_{aj}|\hat{V}^{(cl)}|\chi_{bk}\rangle,$$

if the cluster considered contains both atoms a and b. Therefore, the set of necessary matrix elements for the band structure calculation can be accumulated from the results of several clusters calculations. The advantage of this approach is that the self-consistent field calculations for a cluster is much simpler than for a crystal.

This approach was applied to the ZrO_2 high-temperature cubic phase band structure calculations.[76] Several clusters with Zr border atoms containing neighbors up the fifth order including were calculated with the Coulomb embedding potential. The obtained band structure shown in Figure 14 is in good agreement with obtained in[77] and[78].

Conclusions

In this article, the problem of the embedding potential generation for a ion-covalent crystal is described.

Considering a small system as part of the large system, it is not sufficient to calculate the potential produced by the rest of the large system and to consider the small system in this potential. The state of the small system in this potential will deviate from the state of the small system as part of the large system, because of the difference in boundary conditions. This deviation can be rather large. It is necessary to develop an additional potential and to consider the sum of the additional potential and the potential produced by the rest of the large system as embedding potential. The additional potential should be generated so as to obtain the least possible deviation of the small system in the embedding potential state from the state of the small system as part of the large system.

In this article, this approach is applied to ion-covalent crystals within several approximations imposed to make corresponding equations simpler.

The one-determinant HF approximation was used to describe states of the large system, the small system, and the small system as part of the large system. Here, the one-determinant approximation is important; and the density functional KS equations can be used instead of HF equations. However, the many-determinant approximation can also be used, providing that the number of orbitals which are large in the cluster border region coincide with that in one-determinant approximation; all other orbitals are negligible small in the border region and are designed to improve the wave function inside the cluster. The corresponding equations in this case will be much more elaborated and difficult for numerical calculations.

The valence electrons only approximation was used, assuming that all core states are described with ECP. This approximation is important only for border atoms; for atoms in the inner region, it can be easily removed.

It is easy to override the two atoms and the bonds equivalence assumptions.

The embedding potential has long-range and short-range components. The long-range component in ion-covalent crystals is universal and it can be used with any approximation (one-determinant, many determinant, HF, DFT) used for the cluster wave function. This component generation is described in this article in detail.

To generate the short-range component of the embedding potential, the state of the cluster as part of the crystal was defined in the one-determinant approximation. Equations for cluster in crystal occupied and virtual one-electron orbitals and energies were developed in terms of orbitals and energies of the large system (the finite crystal). Considering these orbitals and energies as predefined, a method was described to generate the short-range component of the embedding potential. This embedding potential possesses the following property: the self-consistent field calculations of the cluster in this embedding potential reproduce exactly the whole set of predefined occupied and virtual orbitals and energies.

For the embedded cluster, it is the occupied and lower virtual states that are important. Thus, the higher virtual states can be modified, providing that the functional space of the cluster occupied and virtual state is the same. With this modification, an embedding potential can be generated to satisfy some auxiliary conditions, if necessary.

The embedding potential was generated with a particular atomic basis set. To apply it to a system with a different atomic basis set, separable potential representation of the embedding potential can be used.

Acknowledgment

This work was done with the support of St. Petersburg State University Computer Center.

Appendix A: Boundary Conditions Transfer

Consider one electron in the periodic potential problem

$$\hat{H}_0\psi(\mathbf{r}) = E\,\psi(\mathbf{r}) \qquad \hat{H}_0 = -\frac{1}{2}\Delta + V_0(\mathbf{r}).$$

The periodic potential $V_0(\mathbf{r})$ is invariant under any translation

$$V_0(\boldsymbol{r}+\boldsymbol{R}_\ell)=V_0(\boldsymbol{r}),$$
$$\boldsymbol{R}_\ell=\ell_1\boldsymbol{a}_1+\ell_2\boldsymbol{a}_2+\ell_3\boldsymbol{a}_3,$$

where $\boldsymbol{R}_\ell$ is the translation vector and $\boldsymbol{a}_1$, $\boldsymbol{a}_2$, $\boldsymbol{a}_3$ are primitive translation vectors. The eigenvalue and eigenfunction problem can be written as

$$\left(-\frac{1}{2}\Delta + V_0(\mathbf{r})\right)\psi_n(\mathbf{k},\mathbf{r}) = E_n(\mathbf{k})\,\psi_n(\mathbf{k},\mathbf{r}),$$

where $\boldsymbol{k}$ is the wave vector in the first Brillouin zone and n is the band number. The eigenfunctions $\psi_n(\mathbf{k},\mathbf{r})$ are Bloch functions

$$\psi_n(\mathbf{k},\mathbf{r}+\boldsymbol{R}_\ell) = e^{i(\boldsymbol{k},\boldsymbol{R}_\ell)}\,\psi_n(\mathbf{k},\mathbf{r}),$$

normalized to δ-function

$$\int \psi_n^*(\mathbf{k},\mathbf{r})\,\psi_m(\mathbf{k}',\mathbf{r})\,d^3r = \delta_{nm}\,\delta(\mathbf{k}-\mathbf{k}').$$

In this case, the Green function is

$$G_0(\mathbf{r},\mathbf{r}';E) = \sum_n \int_{BZ} \frac{\psi_n(\mathbf{k},\mathbf{r})\psi_n^*(\mathbf{k},\mathbf{r}')}{E-E_n(\mathbf{k})}\,d^3k.$$

where integral over $\boldsymbol{k}$ is over the first Brillouin zone and the sum over n is over all bands. The Green function G_0 satisfies equations

$$\left(-\frac{1}{2}\Delta + V_0(\mathbf{r}) - E\right)G_0(\mathbf{r},\mathbf{r}';E) = -\delta^3(\mathbf{r}-\mathbf{r}'), \qquad \text{(A.1.1)}$$

$$\left(-\frac{1}{2}\Delta + V_0(\mathbf{r}) - E\right)G_0(\mathbf{r}',\mathbf{r};E) = -\delta^3(\mathbf{r}-\mathbf{r}'). \qquad \text{(A.1.2)}$$

Now consider a closed surface S, the space Ω from S to infinity, and the equation

$$\left(-\frac{1}{2}\Delta + V_0(\mathbf{r})\right)\psi(\mathbf{r}) = E\,\psi(\mathbf{r}), \qquad \boldsymbol{r}\in\Omega. \qquad \text{(A.2)}$$

It is shown below how zero boundary conditions for ψ at the infinity can be transferred to the surface S. To do this, the surface inverse G_0^{-1} of G_0 is introduced as

$$\int_S G_0^{-1}(\mathbf{r}_s,\mathbf{r}_s'';E)\,G_0(\mathbf{r}_s'',\mathbf{r}_s';E)\,d^2r_s'' = \delta^2(\mathbf{r}_s,\mathbf{r}_s'),$$

where the subscript s means that $\mathbf{r}_s$ belongs to the surface S.

Multiplying Eq. (A.1.2) by $\psi(\mathbf{r})$, Eq. (A.2) by $G_0(\mathbf{r}',\mathbf{r};E)$, subtracting products and integrating the difference over space Ω_2, one obtains

$$\psi(\mathbf{r}') = \frac{1}{2}\int_\Omega \{\psi(\mathbf{r})\,\Delta\,G_0(\mathbf{r}',\mathbf{r};E) - G_0(\mathbf{r}',\mathbf{r};E)\,\Delta\,\psi(\mathbf{r})\}\,d^3r. \qquad \text{(A.3)}$$

This equation can be transformed to the surface integral with the help of Green's theorem

$$\int_\Omega \{U_1\,\Delta\,U_2 - U_2\,\Delta\,U_1\}\,d^3r = \int_S \left\{U_1\,\frac{\partial}{\partial \boldsymbol{n}_s}U_2 - U_2\,\frac{\partial}{\partial \boldsymbol{n}_s}U_1\right\}d^2r_s, \qquad \text{(A.4)}$$

where $\partial/\partial\boldsymbol{n}_s$ is the normal derivative, the normal being external to the volume Ω. Applying (A.4) to Eq. (A.3) one obtains

$$\psi(\mathbf{r}) = \frac{1}{2}\int_S \left\{\psi(\mathbf{r}_s)\,\frac{\partial}{\partial \boldsymbol{n}_s}G_0(\mathbf{r},\mathbf{r}_s;E) - G_0(\mathbf{r},\mathbf{r}_s;E)\,\frac{\partial}{\partial \boldsymbol{n}_s}\psi(\mathbf{r}_s)\right\}d^2r_s,$$

where $\mathbf{n}$ is external to Ω. Function $\psi(\mathbf{r})$ satisfies zero boundary conditions at the infinity. Therefore, surface integral at the infinity vanishes. By reversing the $\boldsymbol{n}$ direction so that it will be internal to Ω and by placing $\mathbf{r}$ on the surface, one obtains

$$\psi(\mathbf{r}_s) = \frac{1}{2}\int_S \left\{G_0(\mathbf{r}_s,\mathbf{r}_s';E)\,\frac{\partial}{\partial \boldsymbol{n}_s'}\psi(\mathbf{r}_s') - \psi(\mathbf{r}_s')\,\frac{\partial}{\partial \boldsymbol{n}_s'}G_0(\mathbf{r}_s,\mathbf{r}_s';E)\right\}d^2r_s'. \qquad \text{(A.5)}$$

This is a relation between $\psi(\mathbf{r}_s)$ on the surface and its normal derivative $\partial\psi/\partial\boldsymbol{n}_s$. Let us rewrite it. For this, we replace $\mathbf{r}_s$ in the Eq. (A.5) by $\mathbf{r}_s''$, multiply both sides by $G_0^{-1}(\mathbf{r}_s,\mathbf{r}_s'';E)$ and integrate over $\mathbf{r}_s''$. The result is

$$\frac{1}{2}\frac{\partial}{\partial \boldsymbol{n}_s}\psi(\mathbf{r}_s) = \int_S G_0^{-1}(\mathbf{r}_s,\mathbf{r}_s';E)\,\psi(\mathbf{r}_s')\,d^2r_s'$$
$$+\frac{1}{2}\int_S \left\{\int_S G_0^{-1}(\mathbf{r}_s,\mathbf{r}_s'';E)\,\frac{\partial}{\partial \boldsymbol{n}_s'}G_0(\mathbf{r}_s'',\mathbf{r}_s';E)\,d^2r_s''\right\}\psi(\mathbf{r}_s')\,d^2r_s'.$$

Introducing function

$$U(\mathbf{r}_s,\mathbf{r}_s';E) = G_0^{-1}(\mathbf{r}_s,\mathbf{r}_s';E) + \frac{1}{2}\int_S G_0^{-1}(\mathbf{r}_s,\mathbf{r}_s'';E)\,\frac{\partial}{\partial \boldsymbol{n}_s'}G_0(\mathbf{r}_s'',\mathbf{r}_s';E)\,d^2r_s''$$

one can write

$$\frac{1}{2}\frac{\partial}{\partial \boldsymbol{n}_s}\psi(\mathbf{r}_s) = \int_S U(\mathbf{r}_s,\mathbf{r}_s';E)\,\psi(\mathbf{r}_s')\,d^2r_s'. \qquad \text{(A.6)}$$

Any solution of Eq. (A.2) with zero boundary conditions at the infinity must satisfy the Eq. (A.6). This equation is the nonlocal form of an ordinary boundary condition relating the value of the derivative of a function at the boundary to the value of the function at the boundary.

Appendix B: Adams-Gilbert Equations

In what follows the many-electron system is considered in one determinant approximation. In this case, the system of HF equations for spin-orbitals can be obtained where each equation has form of eigenfunction and eigenvalue equation with one common operator (Fock operator) in each equation. This form of HF equations is usually referred to as canonical equations and the eigenfunctions of Fock operator are referred to as canonical spin-orbitals. However, instead the canonical spin-orbitals their linear combinations can be used, which are referred to as noncanonical spin-orbitals. Sometimes the noncanonical spin-orbitals are preferable, because they are easier to calculate, or because they provide simpler physical interpretation of results.

In the next section, equations for noncanonical spin-orbitals are derived and in the following section auxiliary conditions are discussed.

Noncanonical spin-orbitals equations

In this section, equations for noncanonical spin-orbitals are obtained using the total energy minimization without imposing any orthonormality condition. The one-determinant approximation is used. Canonical spin-orbitals are denoted as $\psi_p(x)$, $p=1,\ldots,N$, where N is the number of electrons. The noncanonical spin-orbitals (linear combinations of canonical spin-orbitals) are denoted as $\varphi_q(x)$. The noncanonical spin-orbitals are assumed to be linearly independent, because otherwise the one-determinant wave functions is identically equal to zero, but they are not assumed to be orthonormal. The total energy of many-electron system is

$$E=\int\left[\hat{h}(x)\rho(x|x')\right]_{x'=x}dx+\frac{1}{2}\int g(x_1,x_2)\rho(x_1,x_2|x_1,x_2)dx_1dx_2,$$

where $\hat{h}(x)$ is one-electron operator (kinetic energy and the energy in the external potential), $g(x_1,x_2)$ is the electron-electron interaction energy operator,

$$\rho(x|x')=\sum_{p=1}^{N}\psi_p(x)\psi_p^*(x')=\sum_{p,q=1}^{N}\varphi_p(x)(S^{-1})_{pq}\varphi_q^*(x')$$

is the first-order reduced density matrix,

$$\rho(x_1,x_2|x_1',x_2')=\rho(x_1|x_1')\rho(x_2|x_2')-\rho(x_1|x_2')\rho(x_2|x_1')$$

is the second-order reduced density matrix, and

$$S_{pq}=\int\varphi_p^*(x)\varphi_q(x)dx$$

is the noncanonical orbitals overlap integral. With the help of noncanonical spin-orbitals the equation for the system total energy can be written as

$$E=\sum_{p,q=1}^{N}(S^{-1})_{qp}H_{pq}+\frac{1}{2}\sum_{p,q,l,m=1}^{N}(S^{-1})_{pq}(S^{-1})_{lm}\left[G_{mq,lp}-G_{mq,pl}\right],$$

where the following notations are used

$$H_{pq}=\int\varphi_p^*(x)\hat{h}(x)\varphi_q(x)dx$$

and

$$G_{mq,lp}=\int\varphi_m^*(x)\varphi_q^*(x')g(x,x')\varphi_l(x)\varphi_p(x')dxdx'.$$

The equations for noncanonical spin-orbitals are Euler equations for the functional E without any imposed auxiliary conditions

$$\frac{\delta}{\delta\varphi_j^*}E=0,\quad j=1,2,\ldots,N, \tag{B.1}$$

where $\delta/\delta\varphi$ denotes the variational derivative. The variational derivative over φ_j^* only is used because variational derivative over φ_j will yield the same equations but complex conjugate. Taking into account the $G_{qm,pl}=G_{mq,lp}$ equality the following equation can be obtained

$$\begin{aligned}\frac{\delta}{\delta\varphi_j^*}E=&\sum_{p,q=1}^{N}(S^{-1})_{qp}\frac{\delta}{\delta\varphi_j^*}H_{pq}\\&+\frac{1}{2}\sum_{p,q,l,m=1}^{N}(S^{-1})_{pq}(S^{-1})_{lm}\frac{\delta}{\delta\varphi_j^*}\left[G_{mq,lp}-G_{mq,pl}\right]\\&+\sum_{p,q=1}^{N}\left[\frac{\delta}{\delta\varphi_j^*}(S^{-1})_{pq}\right]\left[H_{pq}+\sum_{l,m=1}^{N}(S^{-1})_{lm}\left(G_{mq,lp}-G_{mq,pl}\right)\right].\end{aligned}$$

One has

$$\frac{\delta}{\delta\varphi_j^*}H_{pq}=\delta_{jp}\hat{h}(x)\varphi_q(x)$$

and

$$\begin{aligned}\frac{1}{2}\sum_{p,q=1}^{N}(S^{-1})_{pq}\sum_{l,m=1}^{N}(S^{-1})_{lm}\frac{\delta}{\delta\varphi_j^*}\left[G_{mq,lp}-G_{mq,pl}\right]&\\=\sum_{q=1}^{N}(S^{-1})_{qj}\left[\hat{J}(x)-\hat{K}(x)\right]\varphi_q(x),&\end{aligned}$$

where $\hat{J}(x)$ and $\hat{K}(x)$ are Coulomb and exchange operators

$$\begin{aligned}\hat{J}(x)&=\int\rho(x'|x')g(x,x')dx',\\\hat{K}(x)f(x)&=\int\rho(x|x')g(x,x')f(x')dx'.\end{aligned}$$

To find the variational derivative of the inverse matrix, one can use the equation

$$S^{-1}S=I.$$

Hence,

$$\frac{\delta}{\delta\varphi_j^*}\left(S^{-1}S\right)=0$$

and

$$\frac{\delta}{\delta\varphi_j^*}S^{-1}=-S^{-1}\left(\frac{\delta}{\delta\varphi_j^*}S\right)S^{-1}.$$

Therefore,

$$\frac{\delta}{\delta\varphi_j^*}\left(S^{-1}\right)_{pq}=-\sum_{l=1}^{N}\left(S^{-1}\right)_{pj}\varphi_l(x)\left(S^{-1}\right)_{lq}.$$

Besides,

$$\sum_{l,m=1}^{N}\left(S^{-1}\right)_{lm}\left(G_{mq,lp}-G_{mq,pl}\right)=\int\varphi_q^*(x)\left[\hat{J}(x)-\hat{K}(x)\right]\varphi_p(x)dx.$$

With the help of these equations, system (B.1) can be written as

$$\sum_{q=1}^{N}\left(S^{-1}\right)_{qj}\left[\hat{F}(x)\varphi_q(x)-\sum_{l,m=1}^{N}\varphi_l(x)\left(S^{-1}\right)_{lm}F_{mq}\right]=0, \qquad \text{(B.2)}$$

where

$$\hat{F}(x)=\hat{h}(x)+\hat{J}(x)-\hat{K}(x)$$

is the Fock operator and

$$F_{mq}=\int\varphi_m^*(x)\hat{F}(x)\varphi_q(x)dx$$

is the Fock operator matrix element.

The density operator $\hat{\rho}(x)$ is defined by the following equation

$$\hat{\rho}(x)f(x)=\int\rho(x|x')f(x')dx'. \qquad \text{(B.3)}$$

One can use the equation

$$\begin{aligned}&\hat{\rho}(x)\hat{F}(x)\hat{\rho}(x)\varphi_q(x)=\hat{\rho}(x)\hat{F}(x)\varphi_q(x)\\&=\int\rho(x|x')\hat{F}(x')\varphi_q(x')dx'=\sum_{l,m=1}^{N}\varphi_l(x)\left(S^{-1}\right)_{lm}F_{mq}.\end{aligned} \qquad \text{(B.4)}$$

Equation (B.2) can be written as

$$\sum_{q=1}^{N}\left(S^{-1}\right)_{qj}\left[\hat{F}(x)\varphi_q(x)-\hat{\rho}(x)\hat{F}(x)\hat{\rho}(x)\varphi_q(x)\right]=0 \qquad \text{(B.5)}$$

after its second term transformation with the help of (B.4). Multiplying (B.5) by S_{jp} and calculating the sum over j one obtains

$$\begin{aligned}&\sum_{q=1}^{N}\left(\sum_{j=1}^{N}\left(S^{-1}\right)_{qj}S_{jp}\right)\left[\hat{F}(x)\varphi_q(x)-\hat{\rho}(x)\hat{F}\hat{\rho}(x)\varphi_q(x)\right]\\&=\sum_{q=1}^{N}\delta_{qp}\left[\hat{F}(x)\varphi_q(x)-\hat{\rho}(x)\hat{F}(x)\hat{\rho}(x)\varphi_q(x)\right]=0.\end{aligned}$$

Therefore, the system of equations for noncanonical spin-orbitals can be written as

$$\hat{F}(x)\varphi_q(x)=\hat{\rho}(x)\hat{F}(x)\hat{\rho}(x)\varphi_q(x), \quad q=1,2,\ldots,N. \qquad \text{(B.6)}$$

Auxiliary conditions

Although Eqs. (B.6) are written as equations for occupied spin-orbitals φ_q these equations defines not the particular noncanonical orbitals, but the N-dimensional functional space $\mathcal{R}_N$. It becomes evident when Eq. (B.6) is written as

$$\left(\hat{F}(x)-\hat{\rho}(x)\hat{F}(x)\hat{\rho}(x)\right)\varphi_q(x)=0, \quad q=1,2,\ldots,N. \qquad \text{(B.7)}$$

All occupied noncanonical spin-orbitals are eigenfunctions of one operator in the left-hand side of (B.7) with the same eigenvalue equal to zero.

Suppose that the functional space $\mathcal{R}_N$ is found, and we are looking for N particular noncanonical spin-orbitals φ_k in this space, which are normalized to 1

$$\int|\varphi_k(x)|^2dx=1, \qquad k=1,2,\ldots,N$$

and provide the extremum to the functional

$$W=\sum_{k=1}^{N}\int\varphi_k^*(x)\hat{w}(x)\varphi_k(x)dx,$$

where $\hat{w}(x)$ is a Hermitian operator. The normalization condition can be taken into account with Lagrange multipliers λ_k and one arrives at the stationary state problem with functional

$$W'=\sum_{k=1}^{N}\int\varphi_k^*(x)(\hat{w}(x)-\lambda_k)\varphi_k(x)dx.$$

The condition that spin-orbitals belong to the functional space $\mathcal{R}_N$ can be taken into account using the density operator $\hat{\rho}(x)$ (B.3) as the projector onto $\mathcal{R}_N$

$$\varphi_k(x)=\hat{\rho}(x)f_k(x), \qquad \text{(B.8)}$$

where $f_k(x)$ are spin-orbitals on which no conditions are imposed except their square modulus integrability. Then the functional is obtained

$$W'=\sum_{k=1}^{N}\int(\hat{\rho}f_k)^*(\hat{w}-\lambda_k)\hat{\rho}f_k(x)dx=\sum_{k=1}^{N}\int f_k^*\hat{\rho}(\hat{w}-\lambda_k)\hat{\rho}f_k(x)dx$$

and annulling its functional derivatives

$$\frac{\delta}{\delta f_k^*}W'=0$$

the system of equations for $f_k(x)$ are obtained

$$\hat{\rho}(\hat{w}-\lambda_k)\hat{\rho}f_k=0, \qquad k=1,2,\ldots,N.$$

Taking into account the Eq. (B.8), this equation can be written as the following equation for $\varphi_k(x)$

$$\hat{\rho}\hat{w}\hat{\rho}\varphi_k=\lambda_k\varphi_k. \tag{B.9}$$

At the same time, any $\varphi_k(x)$ belonging to $\mathcal{R}_N$ obeys the equation

$$\hat{F}\varphi_k=\hat{\rho}\hat{F}\hat{\rho}\varphi_k.$$

Combining this equation with Eq. (B.9), the system of equations can be obtained

$$\left(\hat{F}+\hat{\rho}\hat{A}\hat{\rho}\right)\varphi_k=\lambda_k\varphi_k, \qquad k=1,2,\ldots,N, \tag{B.10}$$

where

$$\hat{A}=\hat{w}-\hat{F}.$$

The system of Eq. (B.10) is known as Adams–Gilbert equations.

Appendix C: Ewald Potential

The potential due to the finite system of point charges is considered

$$V(\boldsymbol{r})=\sum_n^N \frac{e_n}{|\boldsymbol{r}-\boldsymbol{R}_n|}.$$

The Ewald method[60] is based on the identity

$$\frac{1}{r}=\frac{2}{\sqrt{\pi}}\left\{\int_0^G e^{-x^2r^2}dx+\int_G^\infty e^{-x^2r^2}dx\right\},$$

where $G>0$ is any positive constant. With the help of this equation, the potential can be written as a sum of two components

$$V(\mathbf{r})=V_1(\mathbf{r})+V_2(\mathbf{r})$$

with

$$V_1(\mathbf{r})=\frac{2}{\sqrt{\pi}}\sum_{n=1}^N e_n\int_0^G e^{-x^2|\mathbf{r}-\mathbf{R}_n|^2}dx \tag{C.1}$$

and

$$V_2(\mathbf{r})=\frac{2}{\sqrt{\pi}}\sum_{n=1}^N e_n\int_G^\infty e^{-x^2|\mathbf{r}-\mathbf{R}_n|^2}dx. \tag{C.2}$$

Because the sum over n is finite the sum and integral can be interchanged and the Eq. (C.1) for V_1 can be written as

$$V_1(\mathbf{r})=\frac{2}{\sqrt{\pi}}\int_0^G\sum_{n=1}^N e_n e^{-x^2|\mathbf{r}-\mathbf{R}_n|^2}dx. \tag{C.3}$$

Now it is assumed that charges make an infinite periodic lattice so that the position vector $\mathbf{R}_n$ is the sum of the lattice vector $\mathbf{R}_k$, and the position in the unit cell vector $\boldsymbol{\rho}_j$, and charges e_n are the unit cell charges e_j. Applying Eqs. (C.2) and (C.3), in this case, one obtains

$$V_1(\mathbf{r})=\frac{2}{\sqrt{\pi}}\int_0^G\sum_k\sum_{j=1}^{n_0} e_j e^{-x^2|\mathbf{r}-\mathbf{R}_k-\boldsymbol{\rho}_j|^2}dx, \tag{C.4}$$

$$V_2(\mathbf{r})=\frac{2}{\sqrt{\pi}}\sum_k\sum_{j=1}^{n_0} e_j\int_G^\infty e^{-x^2|\mathbf{r}-\mathbf{R}_k-\boldsymbol{\rho}_j|^2}dx.$$

This is a redefinition of the potential. One cannot use an infinite series for the potential from the very beginning because in the case of infinite series the sum and integral can be interchanged if and only if the series is convergent and uniformly convergent which is not true for the point ion lattice potential.

The sum in Eq. (C.4) is the periodic function of $\boldsymbol{r}$

$$\Phi(\mathbf{r},x)=\frac{2}{\sqrt{\pi}}\sum_k\sum_{j=1}^{n_0} e_j e^{-x^2|\mathbf{r}-\mathbf{R}_k-\boldsymbol{\rho}_j|^2},$$

which can be expanded into Fourier series

$$\Phi(\mathbf{r},x)=\sum_m{}' \Phi_m(x)\, e^{i(\mathbf{g}_m,\mathbf{r})},$$

where the sum is over the reciprocal lattice and prime by the sum means that term with $m=0$ is absent (the zero Fourier component is equal to zero because of the electrical neutrality condition),

$$\Phi_m(x)=\frac{1}{\Omega}\sum_{j=1}^{n_0} e_j\frac{2}{\sqrt{\pi}}\sum_k\int_\Omega e^{-x^2|\mathbf{r}-\mathbf{R}_k-\boldsymbol{\rho}_j|^2-i(\mathbf{g}_m,\mathbf{r}-\mathbf{R}_k)}d\mathbf{r},$$

where Ω is the lattice unit cell. The integral over unit cell and sum over all unit cells is the integral over the whole space. Hence,

$$\Phi_m(x)=\frac{1}{\Omega}\sum_{j=1}^{n_0} e_j\frac{2}{\sqrt{\pi}}\int e^{-x^2|\mathbf{r}-\boldsymbol{\rho}_j|^2-i(\mathbf{g}_m,\mathbf{r})}d\mathbf{r}.$$

Finally, the equations for the Ewald potential are

$$V_1(\mathbf{r})=\int_0^G\sum_m{}'\Phi_m(x)\,e^{i(\mathbf{g}_m,\mathbf{r})}dx=\frac{\pi}{\Omega G^2}\sum_m{}'\sum_{j=1}^{n_0} e_j e^{i(\mathbf{g}_m,\mathbf{r}-\boldsymbol{\rho}_j)}\frac{e^{-v_m}}{v_m},$$
$$v_m=\frac{g_m^2}{4G^2}$$

and

$$V_2(\mathbf{r})=\sum_k\sum_{j=1}^{n_0} e_j\frac{erfc(G|\mathbf{r}-\mathbf{R}_k-\boldsymbol{\rho}_j|)}{|\mathbf{r}-\mathbf{R}_k-\boldsymbol{\rho}_j|}.$$

Appendix D: Ewald Potential Produced by the LP Unit Cell Additional Charges

In this appendix, it is shown that because of the LP unit cell additional charges specific disposition and the electroneutrality condition (23)

$$\sum_{\boldsymbol{n}\in T_\ell} e(\boldsymbol{n})=0 \tag{D.1}$$

the Ewald potential produced by additional charges alone is identically equal to zero.

Consider the LP unit cell, exclude from it all charges of initial unit cell and leave the additional charges only. The components of the Ewald potential due to resulting unit cell are

$$V_1(\boldsymbol{r})=\frac{4\pi}{\Omega}\sum_m \sum_{n_1,n_2,n_2\in T_\ell} e(n_1,n_2,n_3)\frac{1}{g_m^2} \exp\left(i(\boldsymbol{g}_m,\boldsymbol{r}-\boldsymbol{d}(n_1,n_2,n_3))-\frac{g_m^2}{4G^2}\right), \tag{D.2}$$

and

$$V_2(\boldsymbol{r})=\sum_k \sum_{n_1,n_2,n_2\in T_\ell} e(n_1,n_2,n_3)\,\frac{erfc(G|\boldsymbol{r}-\boldsymbol{R}_k-\boldsymbol{d}(n_1,n_2,n_3)|)}{|\boldsymbol{r}-\boldsymbol{R}_k-\boldsymbol{d}(n_1,n_2,n_3)|}. \tag{D.3}$$

However, in these equations, $\boldsymbol{d}(n_1,n_2,n_3)$ is the translation vector. Hence,

$$\exp(i(\boldsymbol{g}_m,\boldsymbol{d}(n_1,n_2,n_3)))=1. \tag{D.4}$$

Therefore, the first component is

$$V_1(\boldsymbol{r})=\frac{4\pi}{\Omega}\sum_m \sum_{n_1,n_2,n_2\in T_\ell} e(n_1,n_2,n_3)\frac{1}{g_m^2}\exp\left(i(\boldsymbol{g}_m,\boldsymbol{r})-\frac{g_m^2}{4G^2}\right).$$

This absolutely convergent series can be written as a product of two sums, one over m and another over n_1,n_2,n_3, and the sum over n_1,n_2,n_3 is equal to zero because of (23). Consequently, $V_1(\boldsymbol{r})=0$.

In the second component (D.3), one has

$$\boldsymbol{R}_k-\boldsymbol{d}(n_1,n_2,n_3)=\boldsymbol{R}_j.$$

Therefore,

$$V_2(\boldsymbol{r})=\sum_j \sum_{n_1,n_2,n_2\in T_\ell} e(n_1,n_2,n_3)\,\frac{erfc\left(G|\boldsymbol{r}-\boldsymbol{R}_j|\right)}{|\boldsymbol{r}-\boldsymbol{R}_j|}.$$

Again, this absolutely convergent series can be written as a product of two sums, one over j and another over n_1,n_2,n_3, and the sum over n_1,n_2,n_3 is equal to zero. Consequently, $V_2(\boldsymbol{r})=0$.

So the Ewald potential from the LP unit cell additional charges is equal to zero and consequently, Ewald potential produced by the LP unit cell is equal to the Ewald potential produced by the initial unit cell.

Appendix E: Solution of the Equation for the LP Unit Cell Additional Charges

The LP unit cell contains n_0 charges of the initial unit cell and N_ℓ additional charges introduced to make absolutely convergent the series for the point ion lattice electrostatic potential. The positions of additional charges are fixed and their values should be found to annul N_ℓ multipole moments of the LP unit cell. In this appendix, it is shown that the equation for the additional charges can be solved analytically[69] for any lattice and for any value of ℓ.

The LP unit cell multipole moment in Cartesian coordinates is

$$Q(n_1,n_2,n_3)=\sum_{j=1}^{n_0+N_\ell} q_j\rho_{jx}^{n_1}\rho_{jy}^{n_2}\rho_{jz}^{n_3}, \qquad n_1,n_2,n_2\in T_\ell,$$

where q_j is the charge of jth atom in the LP unit cell, and

$$\boldsymbol{\rho}_j=v_{j1}\boldsymbol{a}_1+v_{j2}\boldsymbol{a}_2+v_{j3}\boldsymbol{a}_3 \tag{E.1}$$

is the position vector of jth atom in the LP unit cell. Here, $\boldsymbol{a}_1$, $\boldsymbol{a}_2$, $\boldsymbol{a}_3$ are the initial lattice elementary translation vectors,

$$v_{jk}=(\boldsymbol{\rho}_j,\boldsymbol{b}_k) \tag{E.2}$$

are the jth atom dimensionless coordinates, and

$$\boldsymbol{b}_i=\frac{[\boldsymbol{a}_j,\boldsymbol{a}_k]}{(\boldsymbol{a}_i,\boldsymbol{a}_j\times\boldsymbol{a}_k)}, \qquad i,j,k \text{ is the cycle permutation of } 1,2,3 \tag{E.3}$$

are the reciprocal lattice elementary translation vectors. The atom j in the initial unit cell dimensionless coordinates are in the range

$$0\le v_{jk}\le 1, \qquad k=1,2,3$$

and the dimensionless coordinates of the additional charge $e(n_1,n_2,n_3)$ are integers n_1, n_2, n_3.

Apart from multipole moments in Cartesian coordinates the multipole moments in dimensionless coordinates v_1, v_2, v_3 can be used

$$P(m_1,m_2,m_3)=\sum_{j=1}^{n_0+N_\ell} q_j v_{j1}^{m_1}v_{j2}^{m_2}v_{j3}^{m_3}, \qquad m_1,m_2,m_2\in T_\ell.$$

The multipole moments $Q(n_1,n_2,n_3)$ and $P(m_1,m_2,m_3)$ are connected by linear transformation with nonsingular matrix G

$$Q(n_1,n_2,n_3)=\sum_{m_1,m_2,m_3\in T_\ell} G(n_1,n_2,n_3|m_1,m_2,m_3)P(m_1,m_2,m_3), \quad n_1,n_2,n_2\in T_\ell.$$

Therefore, annulling $Q(n_1,n_2,n_3)$ is equivalent to annulling $P(m_1,m_2,m_3)$ and vice versa. Here the equation

$$P(m_1,m_2,m_3)=0, \qquad m_1,m_2,m_3\in T_\ell \tag{E.4}$$

will be used for the additional charges calculations instead Eqs. (21), corresponding to annulling $Q(n_1,n_2,n_3)$.

The multipole moment $P(m_1, m_2, m_3)$ is the sum of two moments, one due to the initial unit cell charges

$$P_0(m_1, m_2, m_3) = \sum_{j=1}^{n_0} q_j v_{j1}^{m_1} v_{j2}^{m_2} v_{j3}^{m_3}, \tag{E.5}$$

which is known, and another due to additional charges

$$P_1(m_1, m_2, m_3) = \sum_{n_1, n_2, n_3 \in T_\ell} e(n_1, n_2, n_3) n_1^{m_1} n_2^{m_2} n_3^{m_3}. \tag{E.6}$$

Therefore, the Eq. (E.4) can be written as system of linear inhomogeneous equations for charges $e(n_1, n_2, n_3)$

$$\sum_{n_1, n_2, n_3 \in T_\ell} n_1^{m_1} n_2^{m_2} n_3^{m_3} e(n_1, n_2, n_3) = -P_0(m_1, m_2, m_3), \quad m_1, m_2, m_3 \in T_\ell. \tag{E.7}$$

The method of this system solution will be demonstrated in the simple 1-D case. In this case, the system of Eqs. (E.7) reads

$$\sum_{n=0}^{\ell} n^m e(n) = -P_0(m), \qquad m = 0, \ldots, \ell. \tag{E.8}$$

The first equation here, corresponding to $m = 0$ and describing the LP unit cell electroneutrality condition,

$$\sum_{n=0}^{\ell} e(n) = -P_0(0) \tag{E.9}$$

is exceptional because the charge $e(0)$ enters only this equation. It is expedient to solve at the beginning the system of all equations except the first one and then to calculate $e(0)$ from the first equation. The system of all equations except the first one can be written as

$$\sum_{n=1}^{\ell} T_{mn} e(n) = -P_0(m), \qquad m = 1, \ldots, \ell, \tag{E.10}$$

where

$$T_{mn} = n^m \tag{E.11}$$

is a simple Vandermonde matrix with integer matrix elements. The system of Eqs. (E.10) can be transformed to contain not square but triangular matrix, hence the system of equations can be converted into a recurrence relation.

The said transformation can be made with the help of $\ell \times \ell$ lower triangular matrix G_{km}, each row of which contains particular polynomial expansion coefficients

$$\tilde{G}_k(x) = x(x-1)\cdots(x-k+1) = \sum_{m=1}^{k} G_{km} x^m.$$

It is evident that $G_{11} = 1$. Besides,

$$\tilde{G}_{k+1}(x) = \tilde{G}_k(x)(x-k),$$

or, in the explicit form

$$\sum_{m=1}^{k+1} G_{k+1,m} x^m = \sum_{m=2}^{k+1} G_{k,m-1} x^m - \sum_{m=1}^{k} k G_{k,m} x^m.$$

Therefore,

$$\begin{cases} G_{k+1,1} = -k G_{k,1}, \\ G_{k+1,m} = G_{k,m-1} - k G_{k,m}, & m = 2, \cdots, k, \\ G_{k+1,k+1} = G_{k,k}, \\ k = 1, \cdots, \ell. \end{cases}$$

So all matrix elements $G_{k,m}$ can be easily found.

Multiplying Eq. (E.10) by the matrix G from the left, one obtains the system of equations

$$\sum_{m=1}^{k} \sum_{n=1}^{\ell} G_{km} T_{mn} e(n) = -\sum_{m=1}^{k} G_{km} P_0(m), \qquad k = 1, \ldots, \ell. \tag{E.12}$$

In this equation,

$$f_k = -\sum_{m=1}^{k} G_{km} P_0(m)$$

are known values, and

$$\sum_{m=1}^{k} G_{km} T_{mn} = \sum_{m=1}^{k} G_{km} n^m = G_k(n).$$

However,

$$G_k(n) = n(n-1)\cdots(n-k+1) = \begin{cases} 0 & \text{if } k < n \\ \dfrac{n!}{(n-k)!} & \text{if } k \geq n \end{cases}$$

Therefore, Eq. (E.12) is

$$\sum_{n=k}^{\ell} \frac{n!}{(n-k)!} e(n) = f(k), \qquad k = 1, \cdots, \ell. \tag{E.13}$$

This is the backward recurrence relation. The charge number ℓ is

$$e(\ell) = \frac{f(\ell)}{\ell!}, \tag{E.14}$$

and all charges with numbers from $k = \ell - 1$ to k=1 can be found one by one from the equation

$$e(k) = \frac{1}{k!}\left(f(k) - \sum_{n=k+1}^{\ell} \frac{n!}{(n-k)!} e(n) \right), \qquad k = \ell - 1, \ell - 2, \ldots, 1. \tag{E.15}$$

Finally, the charge $e(0)$ is found from the LP unit cell electrical neutrality condition (E.9) as

$$e(0) = -\sum_{n=1}^{\ell} e(n) \tag{E.16}$$

because $P_0(0)=0$ due to the electrical neutrality of initial unit cell.

In Ref. 69, it is shown that similar equations can be obtained for 2-D and 3-D lattices. The equations are similar to (E.14), (E.15), and (E.16) if proper numeration order is used to arrange all charges of tetrahedron in a one dimensional array $e(n)$.

Keywords: ion-covalent crystal · electronic structure · embedding · cluster

How to cite this article: I. V. Abarenkov, M. A. Boyko. *Int. J. Quantum Chem.* **2016**, *116*, 211–236. DOI: 10.1002/qua.25041

[1] E. Wigner, F. Seitz, *Phys. Rev.*, **1933**, *43*, 804.
[2] E. Wigner, F. Seitz, *Phys. Rev.*, **1934**, *46*, 509.
[3] F. Bloch, *Z Physik* **1928**, *52*, 555.
[4] J. C. Slater, G. F. Koster, *Phys. Rev.* **1954**, *94*, 1498.
[5] C. Herring, *Phys. Rev.* **1940**, *57*, 1169.
[6] J. C. Slater, *Phys. Rev.* **1937**, *51*, 846851.
[7] J. Korringa, *Physica*, **1947**, *13*, 392.
[8] W. Kohn, N. Rostocker, *Phys. Rev.* **1954**, *94*, 1111.
[9] A. J. Bennett, B. McCarrol, R. P. Messmer, *Phys. Rev. B*, **1971**, *3*, 1397.
[10] A. A. Zunger, *J. Phys. C: Solid State Phys.*, **1974**, *7*, 96106.
[11] A. A. Zunger, *J Chem. Phys.*, **1975**, *62*, 18618.
[12] A. M. Dobrotvorskii, R. A. Evarestov, *Phys. Stat. Sol. B*, **1974**, *66*, 83.
[13] A. M. Dobhotvohskii, R. A. Evahestov, *Phys. Stat. Sol. B* **1974**, *64*, 635.
[14] R. A. Evarestov, M. I. Petrashen, E. M. Ledovskaya, *Phys. Stat. Sol. B*, **1975**, *68*, 453.
[15] R. A. Evarestov, M. I. Petrashen, E. M. Ledovskaya, *Phys. Stat. Sol. B*, **1976**, *76*, 377.
[16] C. Pisani, R. Dovesi, C. Roetti, Hartree-Fock Ab Initio Treatment of Crystalline Systems, Lecture Notes in Chemistry, Vol. *48*; Springer-Verlag: Berlin,**1988**.
[17] R. Dovesi, R. Orlando, A. Erba, C. M. Zicovich-Wilson, B. Civalleri, S. Casassa, L. Maschio, M. Ferrabone, M. De La Pierre, P. DArco, Y. Noel, M. Causa, M. Rerat, B. Kirtman, *Int. J. Quantum Chem.*, **2014**, *114*, 1287.
[18] R. Dovesi, V. R. Saunders, C. Roetti, R. Orlando, C. M. Zicovich-Wilson, F. Pascale, B. Civalleri, K. Doll, N. M. Harrison, I. J. Bush, P. DArco, M. Llunell, M. Caus, Y. Nol, CRYSTAL14, CRYSTAL14 User's Manual; University of Torino: Torino, **2014**.
[19] Z. Barandiaran, L. Seijo, *J Chem. Phys.* **1988**, *89*, 5739.
[20] J. L. Pascual, N. Barros, Z. Barandiara, L. Seijo, *J Phys. Chem. A*, **2009**, *113*, 12454.
[21] T. A. Wesolowski, A. Warshel, *J Phys. Chem.*, **1993**, *97*, 8050.
[22] G. Senatore, K. R. Subbaswamy, *Phys. Rev. B*, **1986**, *34*, 5754.
[23] M. D. Johnson, K. R. Subbaswamy, G. Senatore, *Phys. Rev. B*, **1987**, *36*, 9202.
[24] P. Cortona, *Phys. Rev. B*, **1991**, *44*, 8454.
[25] G. F. Koster, J. C. Slater, *Phys. Rev* **1954**, *95*, 1167.
[26] G. F. Koster, *Phys. Rev* **1954**, *95*, 1436.
[27] G. F. Koster, J. C. Slater, *Phys. Rev.*, **1954**, *96*, 1208.
[28] C. Pisani, R. Dovesi, P. Ugliengo, *Phys. Stat. Sol. B*, **1983**, *116*, 249.
[29] C. Pisani, R. Dovesi, P. Ugliengo, *Phys. Stat. Sol. B*, **1983**, *116*, 547.
[30] A. Warshel, M. J. Levitt, *Mol. Biol.*, **1976**, *103*, 227.
[31] Warshel, A., Computer Modeling of Chemical Reactions in Enzymes and Solutions; Wiley: New York, **1992**.
[32] H. Lin, D. G. Truhlar, *Theor. Chem. Acc.* **2007**, *117*, 185.
[33] H. M. Senn, W. Thiel, *Angew Chem. Int. Ed.*, **2009**, *48*, 1198.
[34] A. V. Kimmel, A. L. Shluger, *J. Non Crystal. Solids*, **2009**, *355*, 1103.
[35] K. McKenna, A. L. Shluger, *Phys. Rev. B*, **2009**, *79*, 224116.
[36] D. M. Ramo, P. V. Sushko, J. L. Gavartin, A. L. Shluger, *Phys. Rev. B*, **2008**, *78*, 23, 235432.
[37] D. Muoz Ramo, P. V. Sushko, A. L. Shluger, *Phys. Rev. B* **2012**, *85*, 024120.
[38] A. S. Mysovsky, P. V. Sushko, E. A. Radzhabov, M. Reichling, A. L. Shluger, *Phys. Rev. B*, **2011**, *84*, 064133.
[39] D. M. Ramo, A. L. Shluger, G. Bersuker, *Phy. Rev. B* **2009**, *79*, 035306.
[40] A. L. Shluger, K. P. McKenna, P. V. Sushko, D. M. Ramo, A. V. Kimmel, *Model. Simul. Mater. Sci. Eng.*, **2009**, *17*, 084004.
[41] M. L. Sushko, P. V. Sushko, I. V. Abarenkov, A. L. Shluger, *J Comput. Chem.*, **2010**, *31*, 2955.
[42] T. Trevethan, A. L. Shluger, L. Kantorovich, *J Phys.: Condens. Matter*, **2010**, *22*, 084024.
[43] A. S. P. Gomes, C. R. Jacob, *Annu. Rep. Prog. Chem., Sect. C: Phys. Chem.* **2012**, *108*, 222277.
[44] M. S. Gordon, D. G. Fedorov, S. R. Pruitt, L. V. Slipchenko, *Chem. Rev.*, **2012**, *112*, 632.
[45] T. A. Wesolowski, S. Shedge, X. Zhou, *Chem. Rev.*, **2015**, *115*, 5891.
[46] F. R. Manby, M. Stella, J. D. Goodpaster, T. F. Miller, *J Chem. Theory Comput.*, **2012**, *8*, 2564.
[47] P. Deak, *Phys. Stat. Sol. B.*, **2000**, *217*, 9.
[48] K. Jug, T. Bredow, *J Comput. Chem.*, **2004**, *25*, 1551.
[49] T. Bredow, R. Dronskowski, H. Ebert, K. Jug, *Prog. Solid State Chem.* **2009**, *37*, 7080.
[50] J. E. Inglesfield, *J Phys. C: Solid State Phys.*, **1981**, *14*, 3795.
[51] J. E. Inglesfield, S. Crampin, H. Ishida, *Phys. Rev. B*, **2005**, *71*, 155120.
[52] N. Marzari, A. A. Mostofi, J. R. Yates, I. Souza, D. Vanderbilt, *Rev. Mod. Phys.*, **2012**, *84*, 1419.
[53] W. J. Adams, *Chem. Phys* **1962**, *37*, 9.
[54] O. Danyliv, L. Kantorovich, *Phys. Rev. B*, **2004**, *70*, 075113.
[55] I. V. Abarenkov, M. A. Boyko, P. V. Sushko, *Int. J. Quantum Chem.*, **2013**, *113*, 1868.
[56] W. J. Adams, *Chem. Phys* **1961**, *34*, 89.
[57] T. L. Gilbert, In Molecular Orbitals in Chemistry, Physics and Biology;P.O. Lowdin,B. Pullman, Eds.; Academic: New York, **1964**.
[58] O. Danyliv, L. Kantorovich, F. Cor, *Phys. Rev. B*, **2007**, *76*, 045107.
[59] E. Madelung, *Phys. Z.*, **1918**, *19*, 524.
[60] P. P. Ewald, *Ann. Phys. (Leipzig)* **1921**, *64*, 253.
[61] H. M. Evjen, *Phys. Rev.*, **1932**, *39*, 675.
[62] Frank, F. C., Philos. Mag. Ser., **1950**, *41*, 1287.
[63] I. I. Tupizin, I. V. Abarenkov, *Phys. Stat. Sol. B.*, **1977**, *82*, 99.
[64] J. V. Calara, J. D. Miller, *J Chem. Phys.*, **1976**, *65*, 843.
[65] V. R. Marathe, S. Lauer, A. X. Trautwein, *Phys. Rev. B* **1983**, *27*, 5162.
[66] D. Wolf, *Phys. Rev. Lett.*, **1992**, *68*, 3315.
[67] D. Wolf, P. Keblinski, S. R. Phillpot, J. Eggebrecht, *J Chem. Phys.* **1999**, *110*, 8254.
[68] S. E. Derenzo, M. K. Klintenberg, M. J. Weber, *J Chem. Phys.* **2000**, *112*, 2074.
[69] I. V. Abarenkov, *Phys. Rev. B*, **2007**, *76*, 165127.
[70] P. V. Sushko, I. V. Abarenkov, *J Chem. Theory Comput.* **2010**, *6*, 1323.
[71] O. Danyliv, L. Kantorovich, *J Phys.: Condens. Matter* **2004**, *16*, 7233.
[72] R. S. Mulliken, *J Chem. Phys.* **1949**, *49*, 497.
[73] V. Magnasco, A. Perico, *J Chem. Phys.*, **1967**, *47*, 971.
[74] I. Mayer, *J Phys. Chem.*, **1996**, *100*, 6249.
[75] I. V. Abarenkov, M. A. Boyko, P. V. Sushko, *Int. J. Quantum Chem.*, **2011**, *111*, 2602.
[76] M. A. Boyko, I. V. Abarenkov, *Int. J. Quantum Chem.*, **2013**, *113*, 1877.
[77] R. Orlando, C. Pisani, C. Roetti, E. Stefanovich, *Phys. Rev. B*, **1992**, *45*, 592.
[78] S. Gennard, F. Cora, C. R. A. Catlow, *J Phys. Chem. B*, **1999**, *103*, 10158.

Received: 30 April 2015
Revised: 14 October 2015
Accepted: 15 October 2015
Published online 11 November 2015